Sustainable Earth Resources Communications

Article

A thermodynamic model for predicting carbon dioxide solubility in aqueous sodium chloride solutions using an association equation of state

Wei Xiong[1,2,*], Yu-Long Zhao[1], Lie-Hui Zhang[1], Shao-Mu Wen[3], Yong Hu[3], Hong-Bin Liang[4], Xin Huang[5], Yong-Chao Wang[1], Xiang-Yu Liu[1], Cheng Cao[1], Tao Zhang[1]

[1] National Key Laboratory of Oil and Gas Reservoir Geology and Exploitation, Southwest Petroleum University, Chengdu 610500, China
[2] Institute of Marine Natural Gas Hydrates, Southwest Petroleum University, Chengdu 610500, China
[3] PetroChina Southwest Oil & Gas Field Company, Chengdu 610051, China
[4] School of Petroleum Engineering, Chongqing University of Science & Technology, Chongqing 401331, China
[5] Research Institute of Natural Gas Technology, PetroChina Southwest Oil & Gasfield Company, Chengdu 610100, China

* Correspondence: 18328068580@163.com

Received: July 10, 2026
Revised: August 18, 2026
Accepted: August 21, 2026
Published: August 28, 2026

Cited as:
Xiong, W., Zhao, Y.-L., Zhang, L.-H., Wen, S.-M., Hu, Y., Liang, H.-B., Huang, X., Wang, Y.-C., Liu, X.-Y., Cao, C., et al. A thermodynamic model for predicting carbon dioxide solubility in aqueous sodium chloride solutions using an association equation of state. Sustainable Earth Resources Communications, 2026, 2(3): 92-114. https://doi.org/10.46690/serc.2026.03.01

Abstract: An activity coefficient-fugacity coefficient type thermodynamic model, i.e., CPA-P, based on the cubic-plus-association equation of state (CPA EoS) and Pitzer's activity model, is presented to study the phase behavior of carbon dioxide (CO_2)-water (H_2O) and CO_2-H_2O-sodium chloride (NaCl) systems at 273.15 to 573.15 K, 0.1 to 350 MPa, and 0-6 molality of NaCl. This model involves the hydrogen-bond interactions between H_2O and CO_2 molecules. The vapor-liquid equilibrium condition results in the extended Henry's law for CO_2 and Raoult's law for H_2O. Moreover, the properties of pure water are calculated by the IAPWS-95 EoS to improve the accuracy of the CPA-P model. The activity coefficients of CO_2 and the osmotic coefficient of H_2O are calculated by Pitzer's approach in aqueous electrolyte solution. The average absolute relative deviations (AARDs) of the CPA-P predictions for CO_2 solubility in pure water and aqueous NaCl solutions are 3.53% and 3.50%, respectively.

Keywords: CCS; solubility; CPA equation of state; Henry's law; CO_2-brine mixtures.

1. Introduction

Carbon dioxide (CO_2) capture and storage (CCS) has emerged as a fundamental strategy for mitigating the greenhouse effect and curbing global warming (Xiong et al., 2024; Springer et al., 2012; Xiong et al., 2025b). The CO_2–water (H_2O) and CO_2–H_2O–sodium chloride (NaCl) systems are of critical importance in various engineered geologic processes (Zhao et al., 2025; Zhao et al., 2015c). Accurate thermodynamic models are essential for quantifying CO_2 sequestration efficiency in geological aquifers (Xiong et al., 2025c). Therefore, developing a robust thermodynamic model grounded in extensive experimental data and a sound physical basis is necessary. Previous thermophysical studies have shown that the density and viscosity behaviors of non-ideal liquid mixtures reflect the combined effects of intermolecular interactions and molecular packing or structural changes (Verma et al., 2019). Similar analyses of multicomponent liquid mixtures have further demonstrated that changes in composition and temperature can alter the relative contributions of intermolecular interactions and structural effects (Suman et al., 2020).

Duan and Sun (2003) proposed a model combining Duan's equation of state (EoS) with Pitzer's theory (Duan et al., 1992; Pitzer, 1973) to calculate CO_2 solubility in brine, which also proved reliable for predicting CO_2 solubility in seawater. Subsequently, a simplified version of Duan's model was introduced, employing a non-iterative EoS to compute CO_2 solubility in brine over ranges of 273.15–533.15 K, 0.1–200 MPa, and 0–4.5 mol·kg^{-1} (Duan et al., 2006). Li and Duan (2007) extended this framework to describe the phase behavior of H^+, OH^-, HCO_3^-, and CO_3^{2-} in the CO_2–H_2O–NaCl system at 273–523 K, 0–100 MPa, and NaCl molalities up to 5 mol·kg^{-1}.

Yandy Scientific Press

ISSN: 3104-977X

Later improvements enabled the model to compute CO_2 solubility in brine for fluid inclusions and in aqueous solutions containing $MgSO_4$, $MgCl_2$, K_2SO_4, $CaCl_2$, and KCl (Mao et al., 2013; Shi and Mao, 2017). However, none of these models can be applied to calculate water solubility in the gas phase for the aforementioned systems.

Alternative thermodynamic models have been developed based on the activity coefficient (γ) of the liquid phase and the fugacity coefficient (φ) of the gas phase (Hassanzadeh et al., 2008; Salari et al., 2011; Zhao et al., 2015c; Zirrahi et al., 2010; Zirrahi et al., 2012). Spycher et al. (2003) presented a non-iterative γ–φ model using the Redlich–Kwong (RK) EoS to describe the phase behavior of the CO_2–H_2O system at 285.15–383.15 K and 0.1–60 MPa, and later extended it to compute CO_2 solubility in saline solutions with NaCl molalities up to 6 mol·kg^{-1} (Spycher et al., 2003; 2005). Spycher and Pruess (2010) applied this model to study a geothermal system involving CO_2 injection. Zhao et al. (2015) developed the PSUCO2 model based on Pitzer's formalism (Pitzer, 1991), which was further extended to compute CO_2 solubility in aqueous solutions containing KCl, $MgCl_2$, NaCl, and $CaCl_2$ (Zhao et al., 2015a; 2015b). Springer et al. (2012) introduced a γ–φ phase-equilibrium model using the Soave–Redlich–Kwong (SRK) EoS for CO_2–H_2O–chloride salt systems. Portier and Rochelle (2005) employed the Peng–Robinson (PR) EoS to compute molar volumes and fugacity coefficients in the gas phase for CO_2 solubility in brines. Subsequently, the PR EoS was used to construct γ–φ models for H_2S–brine, SO_2–brine, N_2–brine, CH_4–brine, CO_2–brine, and gas-mixture–brine systems (Ziabakhsh-Ganji and Kooi, 2012; Zirrahi et al., 2012). While these models can predict water content in the gas phase, they do not incorporate more accurate EoS formulations, such as the statistical association fluid theory (SAFT) or the cubic-plus-association (CPA) EoS.

The SAFT family of EoS has been extensively applied to study CO_2 solubility in aqueous solutions (Ji and Zhu, 2012; Sun and Dubessy, 2012; Yan and Chen, 2010; Ji et al., 2005; Jiang et al., 2016; Xu et al., 2017; Sun and Dubessy, 2010). Ji et al. (2005) extended the SAFT1-RPM model to compute phase equilibria of the CO_2–brine system, treating CO_2 and H_2O molecules with 3B and 4C association schemes, respectively. Yan and Chen (2010) combined the PC-SAFT EoS with the eNRTL model to study CO_2 solubility in brine. Sun and Dubessy (2012) used the SAFT-LJ EoS to predict solubility in the CO_2–brine system. Ji and Zhu (2012) investigated vapor–liquid equilibria (VLE) of the H_2S–CO_2–H_2O–NaCl system using the SAFT2 EoS. Jiang et al. (2016) improved the mean spherical approximation to develop the SAFT2-KMSA model, which can describe liquid densities of electrolyte solutions at 298.15–473.15 K. Nevertheless, the prediction accuracy of SAFT-type EoS for CO_2 solubility in pure water and brine generally falls below that of the γ–φ thermodynamic models.

The CPA EoS, introduced by Kontogeorgis et al. (1996), has been widely adopted for predicting phase equilibria in CO_2-H_2O systems (Kontogeorgis et al., 2006a; Kontogeorgis et al., 2006b; Xiong et al., 2020). Ahmadi and Chapoy (2018) proposed a simplified CPA EoS (sCPA-EoS) to compute CO_2 solubility in mixed-salt aqueous solutions, but its accuracy was below that of Duan's model. Chabab et al. (2019) developed an electrolyte PR-CPA EoS (e-PR-CPA) for the CO_2–H_2O–NaCl system, which proved more accurate than Duan's model under geological storage conditions. Xiong et al. presented an electrolyte CPA EoS (e-CPA) that provides a more consistent framework for all phases (Xiong et al., 2023; Xiong et al., 2025a). Bian et al. (2019) constructed the CPA-WS model by combining CPA with the Wong–Sandler mixing rules (Wong and Sandler, 1992) to study mutual solubility in the CO_2–H_2O system and CO_2 solubility in brine.

Existing thermodynamic models have distinct advantages and limitations for CO_2-H_2O-electrolyte systems. Duan/Pitzer-type models (Duan and Sun, 2003; Zirrahi et al., 2012) have been widely used for CO_2 solubility in aqueous electrolyte solutions over broad temperature, pressure, and salinity ranges, and can accommodate different electrolyte compositions. However, these models mainly focus on CO_2 solubility in the aqueous phase and are less suitable for describing mutual CO_2-H_2O solubility. Conventional γ-φ models, such as PSUCO2 (Zhao et al., 2015c), separately describe the gas and aqueous phases and benefit from the established treatment of electrolyte non-ideality by Pitzer's model. Their limitation is that commonly used cubic EoS do not explicitly account for CO_2-H_2O association, which can affect the description of water content in the gas phase. SAFT-type models (Zuo et al., 2024) provide a more detailed molecular description of association and electrolyte effects and can be extended to multicomponent systems, but this generally requires additional interaction parameters and a more involved parameterization procedure. CPA-based models (Xiong et al., 2023; Bian et al., 2019; Coelho et al., 2025) retain the relatively simple cubic-EoS structure while explicitly accounting for molecular association, thereby improving the description of CO_2-H_2O interactions. Nevertheless, extension of CPA to electrolyte systems introduces additional ion–molecule and association parameters, increasing model complexity. Accordingly, an effective thermodynamic framework should capture both CO_2-H_2O association and electrolyte non-ideality without excessive parameterization. To the best of our knowledge, however, no study has yet reported an unsymmetrical framework based on CPA EoS for modeling CO_2 solubility in brine.

In this study, we developed a thermodynamic model, designated CPA-P, by coupling the CPA EoS with Pitzer's activity model for the CO_2-H_2O and CO_2-H_2O-NaCl systems. Compared with conventional γ–φ models based on RK, SRK, or PR equations of state, CPA-P employs the CPA EoS for the gas phase, allowing CO_2-H_2O cross-association to be explicitly considered in the calculation of fugacity coefficients. Compared with existing CPA-based models, CPA-P adopts an unsymmetrical treatment in which the CPA EoS describes molecular association in the gas phase, whereas Pitzer's activity model accounts for electrolyte non-ideality in the aqueous phase. This formulation combines the respective strengths of CPA and Pitzer without requiring a unified CPA-based treatment of both phases.

CPA has been widely applied to model associating CO_2-H_2O systems (Kontogeorgis et al., 2006a;

Kontogeorgis et al., 2006b; Xiong et al., 2020), while Pitzer's formalism has been extensively used to describe electrolyte effects on CO_2 solubility in aqueous solutions (Pitzer, 1991; Zhao et al., 2015c). Compared with PSUCO2 (Zhao et al., 2015c), CPA-P retains the Pitzer treatment of the aqueous electrolyte phase but introduces the CPA association term to account for CO_2-H_2O interactions. In contrast to e-CPA (Xiong et al., 2023; Xiong et al., 2025a) and CPA-WS (Bian et al., 2019), CPA-P assigns the CPA EoS and Pitzer's activity model separately to the gas and aqueous phases. This treatment preserves the description of molecular association by CPA and the established representation of electrolyte non-ideality by the Pitzer model within the same phase-equilibrium calculation. The performance of the CPA-P model is compared with that of the PSUCO2 and CPA-WS models.

2. Review of experimental data

The experimental datasets were collected from published measurements covering the temperature, pressure, and NaCl molality ranges considered in the CPA-P model. When data from different sources were available under comparable conditions, their consistency was examined, and data showing substantial disagreement with other measurements were excluded from model development. The selected data were divided into three groups: CO_2 solubility in the aqueous phase (Table 1), H_2O content in the gas phase (Table 2), and CO_2 solubility in aqueous NaCl solutions (Table 3). Tables 1 and 2 contain 554 and 303 data points, respectively, all of which were used for parameter evaluation of the CO_2-H_2O system. For the CO_2-H_2O-NaCl system, Table 3 contains 1100 data points, of which 376 were used for parameter correlation, and the remaining 724 were used only for model validation. Thus, a total of 1233 data points were used for model development and parameter correlation, while 724 independent data points were retained for validation.

Table 1. AARDs of CO_2 solubility in aqueous phase.

References	*T* (K)	*P* (MPa)	N_p	AARD (%)		
				CPA-P	PSUCO2*	CPA-WS**
Valtz et al. (2004)	278.20-308.20	0.50-7.96	32	5.17	6.36	10.46
Bamberger et al. (2000)	323.15-353.15	4.05-14.11	29	1.27	5.64	2.68
Briones et al. (1987)	323.15	6.82-17.68	7	2.48	3.66	2.53
Tong et al. (2013)	373.15	7.21-27.26	5	2.42	5.44	4.11
Guo et al. (2014)	273.15-573.15	10.00-120.00	89	2.96	5.04	3.27
Hou et al. (2013a)	298.15-423.15	1.09-17.55	30	4.95	6.54	4.68
Liu et al. (2011)	308.20-323.15	2.10-15.99	15	1.59	2.78	5.44
King et al. (1992)	288.15-298.15	6.08-24.32	27	0.47	0.92	2.34
Malinin (1959)	473.15-573.15	9.80-49.03	76	5.80	4.08	3.47
Miiller et al. (1988)	373.15-473.15	0.33-8.11	49	2.76	3.69	12.41
Nighswander et al. (1989)	393.15-473.15	2.04-10.21	25	7.44	9.55	15.49
Prutton and Savage (1945)	393.15	2.33-70.32	12	6.38	6.77	9.62
D'souza et al. (1988)	323.15-348.15	10.13-15.20	4	4.02	1.74	7.04
Sako et al. (1991)	348.15	10.34-15.31	2	7.39	11.59	9.52
Takenouchi and Kennedy (1965)	423.15-573.15	10.00-140.00	35	6.01	6.85	6.21
Toedheide and Franck (1963)	323.15-573.15	20.00-350.00	92	1.98	5.44	3.45
Wiebe and Gaddy (1939)	348.15-373.15	5.07-70.93	16	0.49	4.92	5.73
Wiebe and Gaddy (1940)	323.15	5.07-70.93	9	0.41	2.54	3.68
Overall			554	3.53	5.07	5.14

*N*p: Number of experimental data points evaluated.

$$AARD = \frac{1}{n}\sum_{i=1}^{n}\frac{\left|x_i^{\exp} - x_i^{cal}\right|}{x_i^{\exp}};$$

x^{exp} stands for the experimental solubility of CO_2 in H_2O-rich phase;
x^{cal} stands for the calculated solubility of CO_2 in H_2O-rich phase.
* indicates that the calculated ranges of the PSUCO2 model are 273.15-573.15 K and 0.1-200 MPa.
** indicates that the calculated ranges of the CPA-WS model are 288.15-523.15 K and 0.1-350 MPa.

Table 2. AARD of H_2O content in CO_2-rich phase.

References	*T* (K)	*P* (MPa)	N_p	AARD (%)		
				CPA-P	PSUCO2*	CPA-WS**
Valtz et al. (2004)	278.20-308.20	0.50-7.96	22	11.21	10.51	14.49
Bamberger et al. (2000)	323.15-353.15	4.05-14.11	29	3.85	6.88	3.51
Briones et al. (1987)	323.15	6.82-17.68	7	3.45	10.22	1.91
Dohrn et al. (1993)	323.15	10.10-30.10	3	10.41	12.71	9.04
D'souza et al. (1988)	323.15-348.15	10.13-15.20	4	13.85	17.53	13.10
King et al. (1992)	288.15-308.20	5.17-20.27	35	6.91	19.28	7.52
Malinin (1959)	473.15-573.15	19.61-58.84	34	6.30	6.38	5.52
Miiller et al. (1988)	373.15-473.15	0.33-8.11	49	6.40	6.94	7.88
Toedheide and Franck (1963)	323.15-573.15	20.00-350.00	90	2.52	3.15	4.77
Wiebe and Gaddy (1941)	298.15-348.15	0.10-70.93	30	9.99	15.31	6.24
Overall			303	5.83	8.77	6.65

Table 3. AARD of CO_2 solubility in aqueous NaCl solutions.

References	*T* (K)	*P* (MPa)	m_{NaCl} (mol·kg^{-1} H_2O)	N_p	AARD (%)		
					CPA-P	PSUCO2*	CPA-WS**
Bando et al. (2003)	303.15-333.15	10.00-20.00	0.173-0.529	36	3.72	1.11	2.48
Zhao et al. (2015)	323.15-423.15	15.00	0-6.000	21	3.78	5.79	4.56
Hou et al. (2013b)	323.15-423.15	2.61-18.21	2.500-4.000	36	5.16	5.31	5.06
Kiepe et al. (2002)	313.15-353.15	0.10-10.10	0.520-4.340	64	5.06	5.24	10.63
Koschel et al. (2006)	323.15-373.15	5.00-20.24	1.000-3.000	14	3.31	4.74	3.52
Malinin and Kurovskaya (1975)	298.15-423.15	4.80	0-5.915	16	2.81	3.74	4.80
Malinin and Kurovskaya (1972)	298.15-348.15	4.80	0-4.458	16	9.01	7.67	7.46
Nighswander et al. (1989)	353.15-473.15	2.11-10.03	0.173	34	6.00	5.38	8.43
Rumpf et al. (1994)	313.15-433.15	0.47-9.64	3.997-5.999	63	1.56	7.20	11.45
Takenouchi and Kennedy (1965)	423.15-523.15	10.00-140.00	1.091-4.274	40	7.03	20.96	-
Yan et al. (2011)	323.15-413.15	5.00-40.00	1.000-5.000	36	3.26	5.31	4.64
Messabeb et al. (2016)***	323.15-423.15	4.99-20.23	0-6.000	40	4.34	4.93	7.13
Guo et al. (2016)***	273.15-473.15	10.00-40.00	1.000-5.000	180	3.97	4.50	6.78
Wang et al. (2019)***	303.15-353.15	3.00-30.00	0-3.000	504	2.58	2.48	9.31
Overall				1100	3.50	4.41	8.38

m_{NaCl} is the molality of NaCl in H_2O. ** indicates the calculated ranges of the CPA-WS model are 298.15-413.15 K and 0.1-50 MPa. *** indicates these experimental data are only used to verify the CPA-P model. - indicates the *P*-*T* range of experimental data exceeds the range of calculation of the model.

The experimental data of CO_2 solubility in H_2O in Table 1 are shown in Fig. 1 (**a**). Experimental data measured below 20 MPa account for 55% of the dataset, and 33% of experimental data are below 10 MPa. Moreover, the percentages of pressure at 20-50 MPa, 50-150 MPa, and 150-350 MPa are 26%, 15%, and 4%, respectively. Hence, lots of experimental data belong to the range of low pressures (Bamberger et al., 2000; Briones et al., 1987; D'souza et al., 1988; Hou et al., 2013a; King et al., 1992; Liu et al., 2011; Miiller et al., 1988; Nighswander et al., 1989; Sako et al., 1991; Tong et al., 2013; Valtz et al., 2004). Experimental data at very high pressures were only presented by Toedheide and Franck (1963). The temperature distribution of experimental data is uniform, and the percentages of temperature at 273-323 K, 323-373 K, 373-423 K, 423-473 K, and 473-573 K are 26%, 17%, 14%, 19%, and 24%, respectively. The number of experimental data points for water content in the CO_2-rich phase in Fig. 1 (**b**) is below that of the solubility data in Fig. 1 (**a**). The percentages of pressure at 0-10 MPa, 10-20 MPa, 20-50

MPa, 50-100 MPa, and 100-350 MPa are 37%, 25%, 17%, 9%, and 12%, respectively. The experimental data are scarce at pressures above 20 MPa (Malinin, 1959; Dohrn et al., 1993; Toedheide and Franck, 1963; Wiebe and Gaddy, 1941). Meanwhile, the temperature distribution of experimental data is not uniform, and the percentages of temperature at 273-323 K, 323-373 K, 373-423 K, 423-473 K, and 473-573 K are 36%, 15%, 7%, 14%, and 28%, respectively. Most of the experimental data are concentrated at 273-373 K. The experimental data for the CO_2-H_2O system extend to 573.15 K and 350 MPa, although the available measurements become relatively limited at high pressures, particularly above 150 MPa.

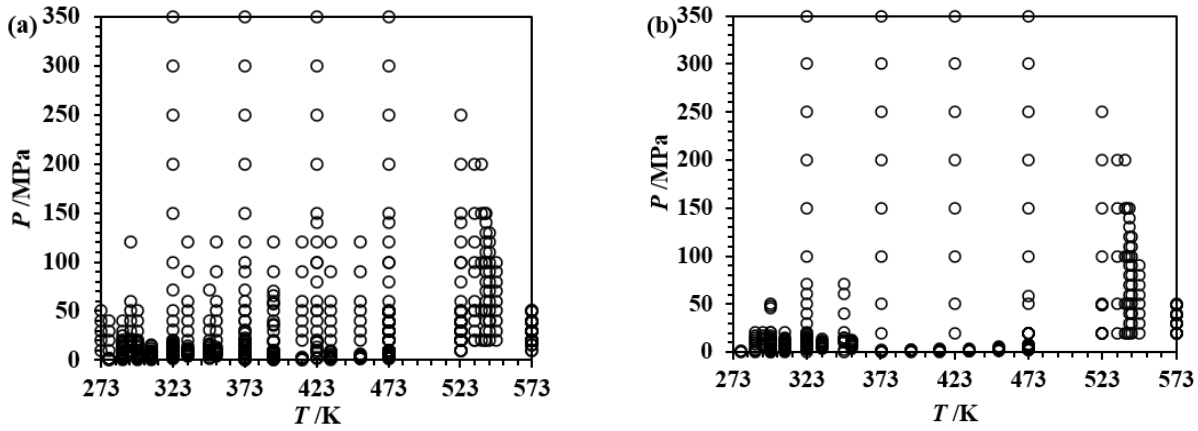

Fig. 1. *P-T* distributions of experimental data of CO_2 solubility in the liquid phase (**a**) and H_2O content in CO_2-rich phase (**b**) at 273.15-573.15 K and 0.1-350 MPa.

The experimental data of carbon dioxide solubility in brine (in Table 3) are shown in Fig. 2. 79% of the experimental data are below 20 MPa, and 48% of the experimental data are below 10 MPa. Most of the experimental data belong to the range of 273.15-323.15 K (43%), and 323.15-373.15 K (39%), and only 8% of experimental data are collected at 423.15-523.15 K. 80% of experimental data is below 3 mol·kg^{-1} in Table 3, including 211 experimental data points at 0 mol·kg^{-1} (Malinin and Kurovskaya, 1972; Malinin and Kurovskaya, 1975; Messabeb et al., 2016; Wang et al., 2019; Zhao et al., 2015c). Fig. 3 indicates that the experimental data of Zhao et al. (2015) are consistent with Hou et al. (2013b) and Messabeb et al. (2016) at 423.15 K. However, the experimental results of Takenouchi and Kennedy (1965) are significantly below those of Zhao et al. (2015) and Messabeb et al. (2016) at 4.274 mol·kg^{-1}, and they are not used in this study. For the CO_2-H_2O-NaCl system, the available experimental data extend to 523.15 K and 140 MPa. Therefore, the range up to 573.15 K and 350 MPa represents the calculation range of the CPA-P model, whereas experimental evaluation of the brine system is limited to the range covered by the available measurements.

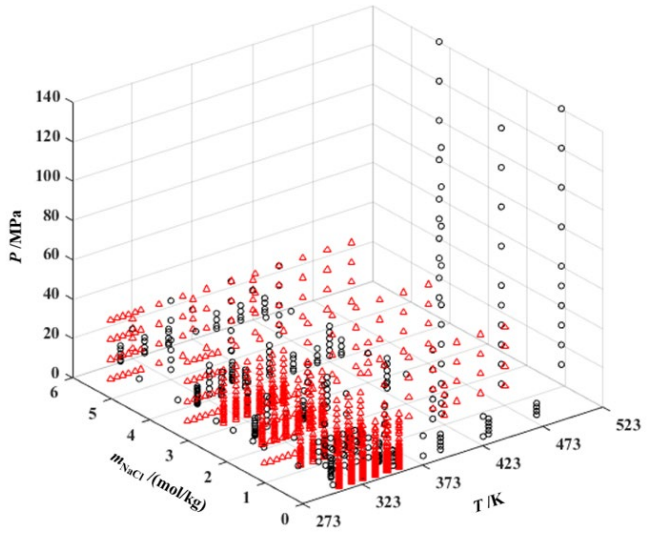

Fig. 2. *P-T-*m_{NaCl} distribution of experimental data of CO_2 solubility in brine at 273.15-523.15 K, 0.1-140 MPa, and 0-6 mol·kg^{-1}. Circles indicate that these experimental data are used to correlate with the CPA-P model. Triangles indicate that these experimental data are only used to verify the CPA-P model.

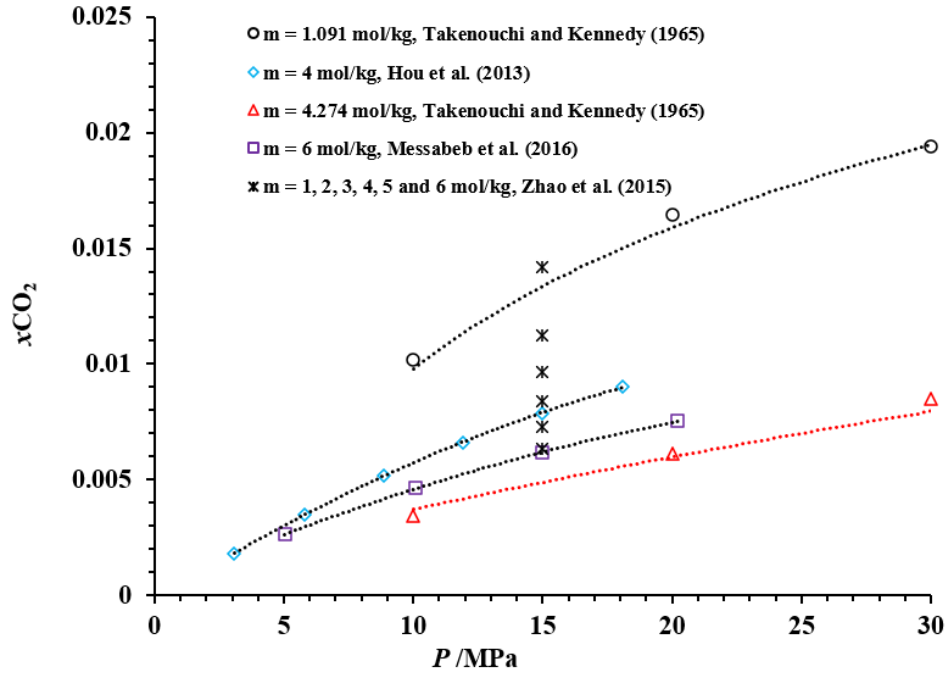

Fig. 3. Experimental data of CO_2 solubility in aqueous NaCl solutions at 423.15 K. Dashed lines refer to trend lines of experimental data. The experimental data points were taken from Takenouchi and Kennedy (1965); Hou et al. (2013b); Messabeb et al. (2016); Zhao et al. (2015).

3. CPA-P approach

3.1. Thermodynamic framework

To model carbon dioxide solubility in aqueous sodium chloride solutions, the reference state is pure liquid for the chemical potential of H_2O at the system temperature and pressure (Rumpf and Maurer, 1993), while the reference state for dissolved CO_2 (Eq. 2) is infinitely diluted gas in pure H_2O at unit molality (Kurz et al., 1996; Pérez-Salado Kamps et al., 2007; Zhao et al., 2015c).

$$\mu_{H_2O} = \mu_{H_2O}^{pure}(T,P) + R \cdot T \cdot ln\left(\gamma_{H_2O} \cdot x_{H_2O}\right) \tag{1}$$

$$\mu_{CO_2} = \mu_{CO_2}\begin{pmatrix} T, P, m_{CO_2} \to 1(\text{amount}), \\ m_{CO_2} \to 0(\text{interraction}) \text{in pure } H_2O \end{pmatrix} + R \cdot T \cdot ln\left(\gamma_{CO_2} \cdot x_{CO_2}\right) \tag{2}$$

where μ_{CO_2} and μ_{H_2O} are respectively the chemical potentials of CO_2 and H_2O; T is system temperature, K; P is system pressure, MPa; x_{CO_2} and x_{H_2O} are respectively the mole fractions of carbon dioxide and water in the liquid phase; m_{CO_2} is molality of CO_2, mol·kg^{-1}; γ_{CO_2} and γ_{H_2O} are the activity coefficients of CO_2 and H_2O, respectively; R is equal to 8.314 MPa·cm^3·mol^{-1}·K^{-1}.

The VLE condition results in the extended Henry's law for carbon dioxide (Eq. 3, Rumpf and Maurer, 1993) and Raoult's law for H_2O (Eq. 4) by using the above reference states (Zhao et al., 2015c).

$$\varphi_{CO_2} y_{CO_2} P = k_{H,CO_2}^0 \, exp\left(\frac{\overline{v}_{CO_2}(P - P_w^s)}{RT}\right) a_{CO_2} \tag{3}$$

$$\varphi_{H_2O} y_{H_2O} P = P_w^s \varphi_w^s \, exp\left(\frac{\overline{v}_w(P - P_w^s)}{RT}\right) a_{H_2O} \tag{4}$$

where φ_{CO_2} and φ_{H_2O} are respectively the fugacity coefficients of carbon dioxide and water, which are calculated by CPA EoS; a_{CO_2} and a_{H_2O} are respectively the activity of carbon dioxide and water; k_{H,CO_2}^0 refers to Henry's constant of CO_2 in pure H_2O (Eq. 5); y_{CO_2} and y_{H_2O} are respectively the mole fractions of carbon dioxide and water in the gas phase; P_w^s and φ_w^s are respectively the vapor pressure and the fugacity coefficient for pure water vapor, which are determined by IAPWS-95 EoS (Wagner and Pruß, 2002); $\overline{v}_w$ is the partial molar volume of liquid H_2O, cm^3·mol^{-1}, which can be approximate by the molar volume of saturated H_2O and calculated by IAPWS-95 EoS; $\overline{v}_{CO_2}$ is the partial molar volume of carbon dioxide, which is determined by fitting experimental data of H_2O-CO_2 system (Tables 1 and 2), and the results are presented in Table 4.

$$ln\left(k_{H,CO_2}^0\right) = \begin{cases} 277.716 - 362.801\left(\frac{T}{T_c}\right) + 57.7716\left(\frac{T_c}{T}\right) + 300.135\, ln\left(\frac{T}{T_c}\right) & 273.15 \le T \le 363.15; P < 2\text{MPa} \\ 7.25021 + 11.5385\left(\frac{T}{T_c}\right) - 15.1174\left(\frac{T_c}{T}\right) - 30.5448\, ln\left(\frac{T}{T_c}\right) & 273.15 \le T \le 573.15; P \ge 2\text{MPa} \end{cases} \tag{5}$$

where T_c is the critical temperature of H_2O (647.096 K).

Table 4. The parameter of $\overline{v}_{CO_2}$ of CPA-P model.

T (K)	*P* (MPa)													
	1	5	10	20	30	40	50	70	100	150	200	250	300	350
273.15	23.0	22.0	21.5	20.9	20.4	20.0	19.6	19.0	18.5	18.3	18.1	17.9	17.7	17.4
278.22	30.0	26.0	24.5	23.8	23.5	23.0	22.5	22.0	21.5	21.3	21.1	20.9	20.7	20.5
288.15	47.0	40.0	33.5	28.8	27.5	26.5	26.0	25.0	24.5	24.3	24.1	23.9	23.7	23.4
293.15	50.0	43.5	36.6	30.1	28.1	27.5	26.3	25.8	25.6	25.4	25.2	25.0	24.8	24.5
298.15	51.0	44.0	36.9	31.9	28.5	27.8	26.7	26.5	26.4	26.2	26.0	25.8	25.6	25.3
308.20	50.0	43.0	36.8	30.0	28.7	28.0	27.1	26.7	26.6	26.4	26.2	26.0	25.8	25.5
323.15	55.0	46.1	40.2	36.9	35.7	34.5	32.6	31.5	30.7	30.3	29.9	29.5	29.1	28.7
333.15	54.0	43.1	38.0	35.5	34.0	33.0	31.0	29.5	29.0	28.8	28.6	28.4	28.2	27.9
348.15	57.0	46.7	43.0	39.7	37.8	36.4	35.5	34.0	33.8	33.5	33.2	32.9	32.6	32.2
353.15	50.0	41.0	39.0	36.5	35.0	34.0	33.0	31.5	30.0	29.6	29.3	29.0	28.7	28.3
373.15	65.0	55.9	46.7	42.0	39.0	37.2	36.0	34.0	32.2	31.7	31.3	30.8	30.4	30.0
393.15	61.0	50.0	44.0	39.9	38.4	37.5	36.2	34.0	32.0	31.5	31.0	30.5	30.0	29.5
413.15	66.0	55.0	43.0	40.0	39.0	38.0	37.1	35.0	33.5	33.0	32.5	32.0	31.5	31.0
423.15	75.0	65.0	55.0	45.0	42.2	40.7	39.5	38.0	36.5	35.0	34.0	33.2	32.4	31.6
433.15	66.0	55.0	48.0	40.3	37.9	36.7	35.4	33.5	32.7	32.2	31.7	31.2	30.8	30.2
453.15	64.0	52.5	45.5	41.0	38.5	36.6	35.6	34.0	32.5	32.0	31.5	31.0	30.5	30.0
473.15	67.0	53.5	45.0	40.3	37.3	36.7	36.0	35.6	35.2	34.9	34.6	34.3	33.8	33.3
523.15			26.4	24.0	22.4	21.4	21.0	21.5	23.5	25.8	27.4	29.4		
533.15				33.9	27.6	23.6	21.3	20.7	21.7	23.1	23.6			
538.15				39.7	28.5	21.1	19.5	21.0	22.0	20.5	16.5			
540.15				39.8	23.0	19.5	20.0	21.0	19.0	17.5				
541.15				40.0	15.2	17.0	18.6	20.5	19.8	13.0				
543.15				42.0	11.9	14.0	16.5	19.3	18.0	14.0*				
548.15				45.0	15.1	15.5	16.6	19.0	13.5					
573.15				46.0	20.8	18.2	20.2							

* indicates that the pressure at this point is 130 MPa.

3.2. Fugacity coefficient of CPA EoS

A two-parameter mixing rule presented by Panagiotopoulos and Reid (1986) is used for the CPA EoS in the Supplementary Materials as follows:

$$\alpha = \sum_i \sum_j y_i y_j \sqrt{\alpha_i \alpha_j}\left(1 - k_{ij} + \left(k_{ij} - k_{ji}\right) y_i\right) \quad (6)$$

$$b = \sum_i x_i b_i \quad (7)$$

where α is the energy parameter of the CPA EoS; b is the co-volume of the CPA EoS; k_{ij} is a binary interaction parameter.

The parameters of k_{ij} and k_{ji} of the CO_2-H_2O system are determined by fitting experimental data in Tables 1 and 2. These parameters are temperature-dependent below 473.15 K (Eqs. 8 and 9). Moreover, the parameters of $k_{CO_2\text{-}H_2O}$ (in Table 5) are temperature-dependent and pressure-dependent above 473.15 K.

$$k_{H_2O\text{-}CO_2} = -0.40141 + 0.0012619T \quad 273.15 \le T \le 573.15 \quad (8)$$

$$k_{CO_2\text{-}H_2O} = -3.844375 + 0.0125T \quad 273.15 \le T \le 473.15 \quad (9)$$

Carbon dioxide is considered a non-self-associating compound (pseudo-associating component), and it has only one electron acceptor (Tsivintzelis et al., 2011). H_2O is modeled using the 4C association scheme. (Wolbach and Sandler, 1998). Hence, the cross-association strength between H_2O and CO_2 can be calculated using the equation proposed by Li and Firoozabadi (2009). A combining rule (Eq. 10) presented by Li and Firoozabadi (2009) is utilized for calculating the cross-association strength with an adjustable parameter (i.e., F), and the values of F (in Table 6) are determined by fitting experimental data in Tables 1-2. The X_{Aj} is calculated by Eq. (11) (Bian et al., 2019).

$$\Delta^{A_i B_j} = F_{ij}\sqrt{\Delta^{A_i B_i}} \quad (10)$$

$$X_{A_j} = \frac{-1 + \sqrt{1 + 4\rho^2 X_{B_i} \Delta^{A_j B_i}}}{2\rho^2 X_{B_i} \Delta^{A_j B_i}} \quad (11)$$

where ρ is the molar density, mol·cm^{-3}; i refers to H_2O; j refers to CO_2; F is the interaction parameter ($F_{ij} = F_{ji}$); XA$_j$ is the approximate mole fraction of carbon dioxide molecules not bonded at site A; A and B stand for bonding sites; Δ^{AiBj} is the association strength.

Table 5. The parameter of $k_{CO_2-H_2O}$ of CPA-P model.

P (MPa)	*T* (K)							
	523.15	**533.15**	**538.15**	**540.15**	**541.15**	**543.15**	**548.15**	**573.15**
20	1.91	1.52	1.56	1.55	1.51	1.48	1.45	1.12
30	1.93	1.66	1.65	1.64	1.65	1.66	1.63	1.43
40	1.91	1.72	1.69	1.68	1.71	1.69	1.65	1.47
50	1.87	1.73	1.68	1.67	1.64	1.61	1.59	1.4
60	1.81	1.70	1.64	1.63	1.59	1.56	1.49	
70	1.75	1.63	1.58	1.56	1.5	1.46	1.41	
80	1.68	1.55	1.50	1.48	1.41	1.38	1.33	
90	1.61	1.46	1.42	1.38	1.35	1.31	1.25	
100	1.56	1.38	1.35	1.29	1.28	1.25	1.17	
110	1.52	1.32	1.29	1.23	1.23	1.18		
120	1.50	1.28	1.25	1.18	1.17	1.13		
130	1.48	1.25	1.21	1.14	1.09	1.09		
140	1.48	1.23	1.19	1.12	1.02			
150	1.47	1.22	1.17	1.10	0.94			
200	1.43	1.17	0.96					
250	1.46							

Table 6. AARD of CO_2 solubility in the pure H_2O phase and water content in the gas phase.

T (K)	*F*	AARD (%)					
		CPA-P		**PSUCO2***		**CPA-WS****	
		x_{CO_2}	y_{H_2O}	x_{CO_2}	y_{H_2O}	x_{CO_2}	y_{H_2O}
273.15	0.00	1.49	--	5.28	--	-	--
278.20	0.00	4.70	17.64	7.52	23.00	-	-
288.15	2.73	2.24	13.83	4.29	23.78	5.62	15.18
293.15	2.91	0.60	7.90	2.87	21.86	2.88	9.07
298.15	2.96	3.33	6.90	4.42	12.97	6.35	5.53
308.20	3.15	2.94	5.64	3.86	8.65	6.23	9.87
323.15	3.46	1.62	6.91	3.20	14.02	3.57	6.09
333.15	3.50	1.40	3.90	5.11	5.72	2.77	3.61
348.15	3.55	2.79	14.09	4.99	20.84	6.63	11.20
353.15	3.60	1.02	3.68	5.82	2.44	3.10	2.81
373.15	4.50	2.07	10.58	5.09	13.66	3.78	6.67
393.15	5.10	4.13	9.68	6.19	3.12	9.39	10.61
413.15	5.70	2.16	2.18	4.94	7.41	3.00	0.77
423.15	6.03	3.09	2.15	5.51	2.60	4.92	1.65
433.15	6.70	3.73	1.84	6.90	12.02	6.45	-
453.15	8.08	2.54	2.77	2.57	13.40	6.53	2.91
473.15	9.64	3.07	6.27	3.77	2.03	6.15	3.98
523.15	12.66	4.67	5.81	5.81	6.31	4.22	5.69
533.15	12.70	4.20	1.18	5.29	0.15	-	-
538.15	13.00	1.60	2.91	5.12	0.24	-	-
540.15	13.03	1.56	1.80	4.79	0.80	-	-
541.15	13.06	3.38	0.34	6.16	0.24	-	-
543.15	13.10	3.62	1.27	6.23	0.31	-	-
548.15	13.20	2.16	0.84	10.94	0.24	-	-
573.15	13.50	13.97	3.84	7.35	4.33	-	-
Overall AARD (%)		3.53	5.83	5.07	8.77	5.14	6.65

F is an interaction parameter of the CPA-P model in the association term. * indicates that the calculated range of the PSUCO2 model is 273.15-573.15 K and 0.1-200 MPa. ** indicates the calculated range of the CPA-WS model is 288.15-523.15 K and 0.1-350 MPa. - indicates the *P-T* range of experimental data exceeds the CPA-WS model. -- indicates a lack of experimental data.

$\varphi_{\mathrm{co_2}}$ and $\varphi_{\mathrm{H_2O}}$ are computed by CPA EoS as follows:

$$\ln\varphi_i = -\ln\left(\frac{v-b}{v}\right)+\frac{b_i}{v-b}-\frac{\alpha}{bRT} \times\left[\frac{\sum_j y_j(\alpha_{ji}+\alpha_{ij})-\sum_j\sum_k y_j^2 y_k(k_{jk}-k_{kj})\sqrt{\alpha_j\alpha_k}+y_i\sum_j y_j(k_{ij}-k_{ji})\sqrt{\alpha_i\alpha_j}}{\alpha}-\frac{b_i}{b}\right] \times\ln\left(\frac{v+b}{v}\right)-\frac{\alpha}{bRT}\left(\frac{b_i}{v+b}\right)+\sum_A^{NS_i}(X_{A_i})-\frac{1}{2}\left(\frac{1.9b_i}{4v-1.9b}\right)\sum_j y_j\sum_A^{NS_j}\left(1-X_{A_j}\right)-\ln Z \tag{12}$$

$$\ln\gamma_{\mathrm{CO_2}} = 2m_{\mathrm{CO_2}}\lambda_{nn}+3m_{\mathrm{CO_2}}^2\mu_{nnn}+2m_{\mathrm{NaCl}}(\lambda_{nc}+\lambda_{na})+6m_{\mathrm{CO_2}}m_{\mathrm{NaCl}}(\mu_{nnc}+\mu_{nna})+m_{\mathrm{NaCl}}^2\xi_{nca} \tag{13}$$

$$\phi-1=\frac{2}{2m_{\mathrm{NaCl}}+m_{\mathrm{CO_2}}}\left\{-A^{\phi}\frac{I^{1.5}}{1+1.2I^{0.5}}+m_{\mathrm{NaCl}}^2\left[\beta_{ca}^{(0)}+\beta_{ca}^{(1)}exp(-2I^{0.5})+2m_{\mathrm{NaCl}}C_{ca}^{\phi}\right]+\frac{1}{2}m_{\mathrm{CO_2}}^2\lambda_{nn} +m_{\mathrm{CO_2}}^3\mu_{nnn}+m_{\mathrm{CO_2}}m_{\mathrm{NaCl}}(\lambda_{nc}+\lambda_{na})+3m_{\mathrm{CO_2}}^2m_{\mathrm{NaCl}}(\mu_{nnc}+\mu_{nna})+m_{\mathrm{CO_2}}m_{\mathrm{NaCl}}^2\xi_{nca}\right\} \tag{14}$$

where subscripts *i*, *j,* and *k* stand for CO_2 or H_2O; *v* is molar volume, $cm^3\cdot mol^{-1}$; NS_i stands for the total number of bonding sites of component *i*; *Z* is the deviation factor.

3.3. Pitzer's activity model

The a_{CO_2} and a_{H_2O} are respectively calculated by Eq. (15) and Eq. (16) (Zhao et al., 2015c).

$$a_{\mathrm{CO_2}} = \gamma_{\mathrm{CO_2}}m_{\mathrm{CO_2}} \tag{15}$$

$$\ln a_{H_2O} = -\frac{\phi M_{H_2O}}{1000}\left(2m_{\mathrm{NaCl}}+m_{\mathrm{CO_2}}\right) \tag{16}$$

where ϕ is the osmotic coefficient of H_2O; M_{H_2O} is molar mass of H_2O, $g\cdot mol^{-1}$; m_{NaCl} is molality of NaCl, $mol\cdot kg^{-1}$.

The $\gamma_{\mathrm{CO_2}}$ (Eq. 13) and ϕ (Eq. 14) can be calculated by Pitzer's approach in aqueous electrolyte solution (Pitzer, 1991; Akinfiev and Diamond, 2010). $\beta_{ca}^{(0)}$, $\beta_{ca}^{(1)}$ and C_{ca}^{ϕ} are Pitzer parameters for NaCl-H_2O system (Pitzer et al., 1984); λ_{nn} and μ_{nnn} are Pitzer interaction parameters of neutral species in Supplementary Materials, their units are $kg\cdot mol^{-1}$ and $kg^2\cdot mol^{-2}$, respectively; λ_{nc} and λ_{na} are Pitzer parameters of ions and neutral species, $kg\cdot mol^{-1}$; μ_{nna}, μ_{nnc} and ξ_{nca} are Pitzer parameters of ions and neutral species, $kg^2\cdot mol^{-2}$; A^{ϕ} and *I* are respectively Debye-Hückel slope for ϕ and ionic strength, which can be calculated by Eqs. (17) and (18).

$$A^{\phi} = \frac{1}{3}(2\pi N_A\rho_w)^{0.5}\left(\frac{e^2}{4\pi\varepsilon_0\varepsilon_r k_B T}\right)^{1.5} \tag{17}$$

$$I = \frac{1}{2}\sum_i m_i z_i^2 \tag{18}$$

where π is Pi (3.14159); N_A is Avogadro constant (6.0221367×10^{23}); ρ_w is the density of H_2O ($kg\cdot m^{-3}$), which can be computed by IAPWS-95 EoS; *e* is elementary charge, and it is equal to 1.60218×10^{-19}; ε_0 and ε_r are the vacuum permittivity (8.85419×10^{-12} $F\cdot m^{-1}$) and the relative permittivity of pure H_2O computed by Fernández et al. (1997) equations; k_B is Boltzmann constant, and it is equivalent to 1.38065×10^{-23} $J\cdot K^{-1}$; z_i is the ionic charge of Na^+ or Cl^-.

The parameter of ξ_{nca} (in Table 7) is determined by fitting experimental data for the CO_2-brine system listed in Table 3. It is primarily influenced by temperature and the molality of NaCl.

3.4. Calculation method

Since the total mole fraction of the gas phase is equal to 1 (Eq. 19), Eqs. (3) and (4) can be combined into Eq. (20).

$$y_{H_2O}+y_{\mathrm{CO_2}} = 1 \tag{19}$$

$$\frac{P_w^s\varphi_w^s\,exp\left(\frac{\overline{v}_w(P-P_w^s)}{RT}\right)a_{H_2O}}{\varphi_{H_2O}P} +\frac{k_{\mathrm{H,CO_2}}^0\,exp\left(\frac{\overline{v}_{\mathrm{CO_2}}(P-P_w^s)}{RT}\right)a_{\mathrm{CO_2}}}{\varphi_{\mathrm{CO_2}}P}-1=0 \tag{20}$$

Eq. (20) can be solved by the Newton-Raphson method with respect to m_{CO2} at a given temperature, pressure, and salt molality. The flow chart is shown in Fig. 4, and the main calculation steps are listed:

Step 1: Input temperature, pressure, and molality of NaCl, and the initial guess of y_{H_2O} is equal to P_w^s/P. Calculate the $\overline{v}_w$, P_w^s and φ_w^s of pure H_2O by using IAPWS-95 EoS. Calculate the interaction parameters of the Pitzer equations. Calculate Henry's constant for CO_2 in pure H_2O.

Step 2: Calculate α and *b* of the CPA EoS for the gas-phase mixture using the mixing rule.

Step 3: Solve the molar volume of the CPA EoS. Calculate $\varphi_{\mathrm{CO_2}}$ and $\varphi_{\mathrm{H_2O}}$.

Step 4: Calculate $a_{\mathrm{CO_2}}$ and a_{H_2O} by Eqs. (13)-(18). Calculate the derivatives of $a_{\mathrm{CO_2}}$ and a_{H_2O} with respect to $m_{\mathrm{CO_2}}$ by Eqs. (S7) and (S8). Update m_{CO2} by the Newton-Raphson method ($m_{\mathrm{CO_2}}^{(new)} = m_{\mathrm{CO_2}}^{(old)} - f(m_{\mathrm{CO_2}})/f'(m_{\mathrm{CO_2}})$).

Step 5: If $|m_{\mathrm{CO_2}}^{(new)}/m_{\mathrm{CO_2}}^{(old)}-1| > 10^{-5}$, then go to Step 4, or else go to Step 6.

Step 6: Obtain $m_{\mathrm{CO_2}}$ and a_{H_2O} from Step 4, and update y_{H_2O} by Eq. (4).

Step 7: If $|y_{\mathrm{H_2O}}^{(new)}/y_{\mathrm{H_2O}}^{(old)}-1| > 10^{-5}$, then go to Step 2, or else output $m_{\mathrm{CO_2}}$ and y_{H_2O}.

Table 7. The parameter of ξ_{nca} of CPA-P model.

T (K)	m_{NaCl} (mol·kg^{-1})						
	0.1	**1**	**2**	**3**	**4**	**5**	**6**
273.15	0.01700	0.00540	0.00302	-0.00180	-0.00217	-0.00270	-0.00410
298.15	0.01888	0.00690	0.00050	-0.00155	-0.00207	-0.00245	-0.00450
303.15	0.01950	0.00750	0.00050	-0.00150	-0.00205	-0.00240	-0.00452
313.15	0.02172	0.00900	0.00100	-0.00140	-0.00200	-0.00230	-0.00450
323.15	0.02527	0.01090	0.00217	-0.00130	-0.00195	-0.00220	-0.00440
333.15	0.02881	0.01490	0.00556	0.00084	-0.00112	-0.00218	-0.00422
348.15	0.03413	0.02090	0.01064	0.00405	0.00013	-0.00215	-0.00380
353.15	0.03590	0.02290	0.01233	0.00512	0.00054	-0.00214	-0.00360
373.15	0.04298	0.03090	0.01910	0.00940	0.00220	-0.00210	-0.00310
393.15	0.07000	0.04840	0.02438	0.01016	0.00240	-0.00100	-0.00210
413.15	0.10000	0.06590	0.02966	0.01093	0.00371	0.00200	-0.00020
423.15	0.14000	0.10300	0.04730	0.01322	0.00660	0.00250	0.00010
433.15	0.19000	0.13026	0.05200	0.01600	0.00700	0.00300	0.00050
473.15	0.26000	0.18900	0.07500	0.03000	0.01500	0.00800	0.00200
523.15	0.35000	0.27200	0.13000	0.07000	0.04600	0.02600	0.00600
573.15	0.40000	0.32000	0.17000	0.10000	0.07200	0.04200	0.00900

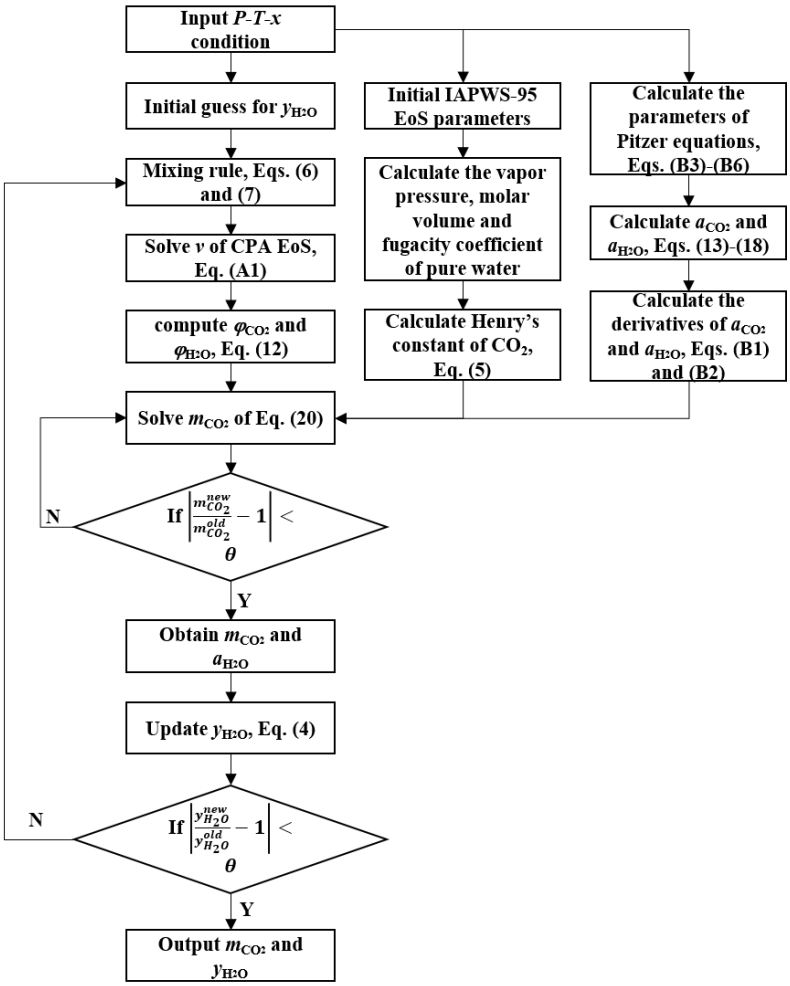

Fig. 4. The flow chart of the CPA-P model. θ is the convergence criterion (10^{-5}).

4. Results and Discussion

4.1. Parameter evaluation

There are five adjustable parameters ($\overline{v}_{CO_2}$, $k_{CO_2-H_2O}$, $k_{H_2O-CO_2}$, *F*, and ξ_{nca}) in the CPA-P model. The data in Tables 1 and 2 are used to determine the parameters for the CO_2-H_2O system. For the CO_2-H_2O-NaCl system, the datasets reported by Messabeb et al. (2016), Guo et al. (2016), and Wang et al. (2019), comprising 724 data points, are reserved for model verification. These datasets were selected as independent literature sources covering different temperature, pressure, and NaCl molality ranges. The remaining 376 data points in Table 3 are used for parameter fitting. The 724 verification data points are not involved in the fitting procedure, and the fitted parameters are kept unchanged during model verification. For the CO_2-H_2O system, $\overline{v}_{CO_2}$, $k_{CO_2-H_2O}$, $k_{H_2O-CO_2}$, and *F* were empirically evaluated using the experimental data listed in Tables 1 and 2. The results show that $k_{H_2O-CO_2}$ is a function of temperature, and its value is therefore regressed using Eq. (8). After $k_{H_2O-CO_2}$ is determined, $k_{CO_2-H_2O}$ is evaluated and regressed using Eq. (9). Finally, *F*, $\overline{v}_{CO_2}$, and ξ_{nca} are successively determined. Some of these parameters depend on temperature, pressure, and NaCl molality, and cubic spline interpolation is used to determine their values over the temperature range of 273.15–573.15 K, pressure range of 0.1-350 MPa, and NaCl molality range of 0–6 mol·kg^{-1}.

4.2. CO_2-H_2O system

The PSUCO2 (Zhao et al., 2015c) and CPA-WS (Bian et al., 2019) models are used to compare with the CPA-P model. The temperature and pressure ranges of the PSUCO2 model for the CO_2-H_2O system are 273.15-573.15 K and 0.1-200 MPa, while the ranges for the CPA-WS model are from 288.15 to 523.15 K and 0.1 to 350 MPa.

Fig. 5 shows that CPA-P and CPA-WS models can accurately calculate the phase behavior of both CO_2 solubility in the liquid phase (Fig. 5**a**, **c**, **e**, and **g**) and H_2O content in the gas phase (Fig. 5**b**, **d**, **f**, and **h**) up to 350 MPa, while the CPA-P model is more accurate at 423.15 K to 473.15 K. Moreover, the CPA-P model is more accurate than the PSUCO2 model at pressures above 100 MPa (Fig. 5**b**, **d**, and **g**), and the predictions of the PSUCO2 model are not consistent with experimental data at 323.15 K and pressures above 70 MPa.

The sensitivity of the CPA-P predictions to the adjustable parameters is not uniform for different phase-equilibrium properties. The calculated H_2O content in the gas phase is particularly sensitive to the binary interaction parameter $k_{CO_2-H_2O}$ and the association parameter F, both of which directly affect the CO_2-H_2O interactions represented by the CPA EoS. In contrast, CO_2 solubility in the aqueous phase is more strongly influenced by $\overline{v}_{CO_2}$ than by these CPA interaction parameters. The influence of the binary interaction parameters also varies with thermodynamic conditions. Both $k_{CO_2-H_2O}$ and $k_{H_2O-CO_2}$ are treated as temperature-dependent parameters, and $k_{CO_2-H_2O}$ is additionally pressure-dependent above 473.15 K. These results indicate that the CPA-P predictions, particularly the calculated H_2O content in the gas phase, are sensitive to the binary interaction and association parameters, and their temperature and pressure dependence must therefore be considered over the investigated range.

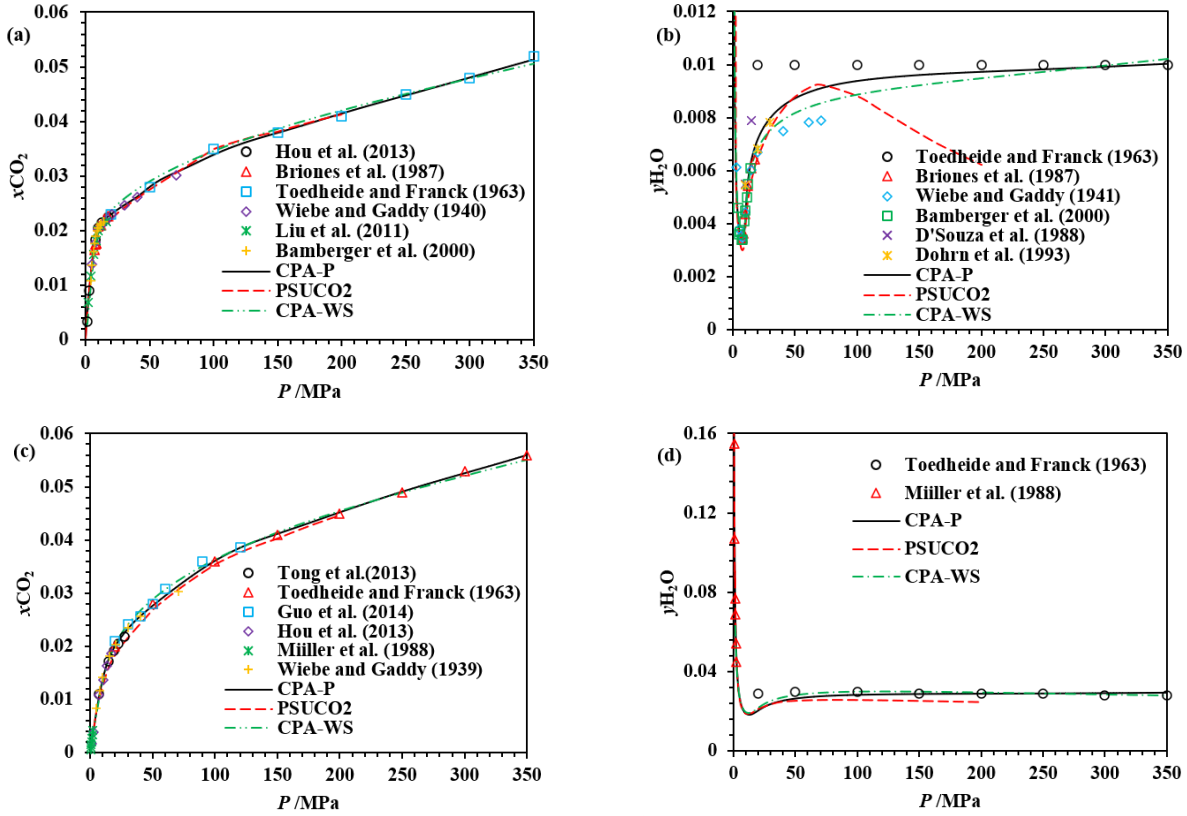

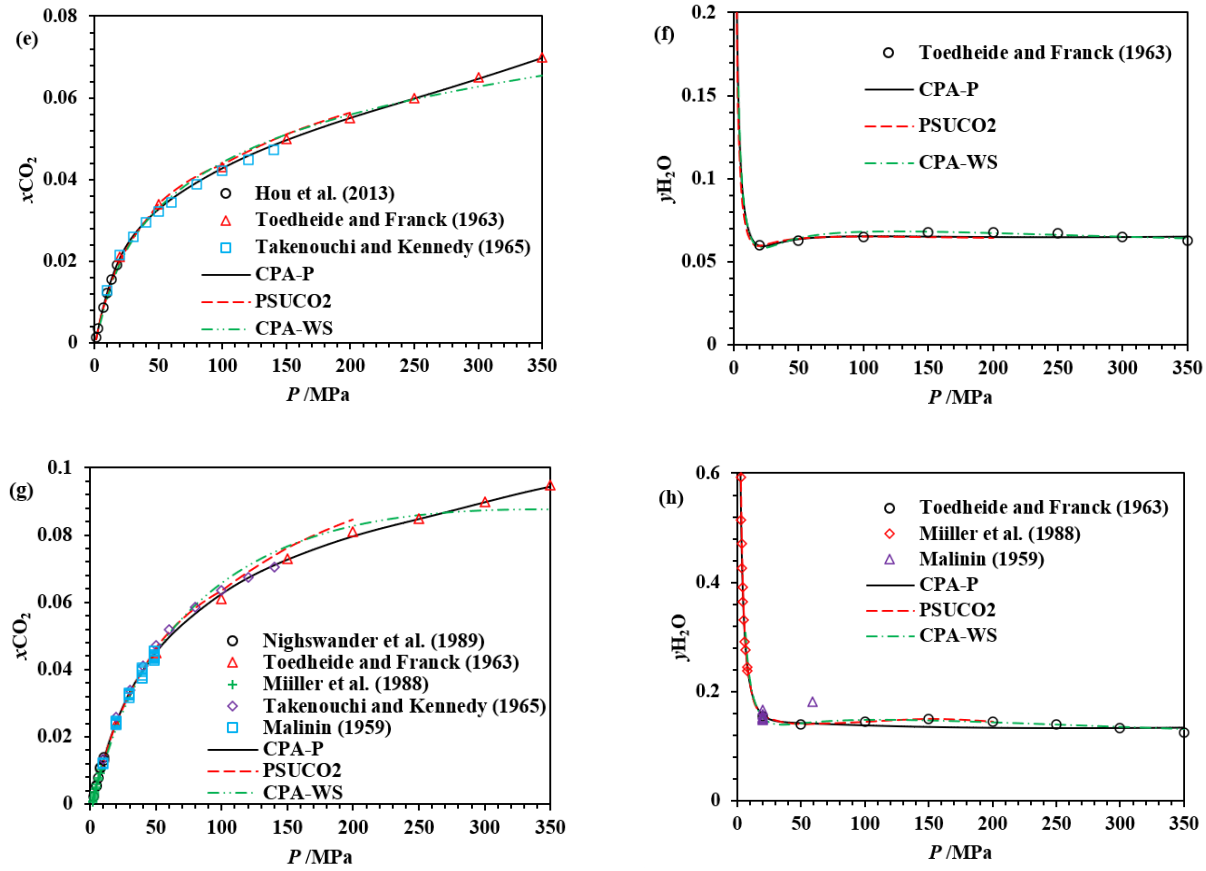

Fig. 5. CO_2-H_2O VLE at 323.15 K (**a** and **b**), 373.15 K (**c** and **d**), 423.15 K (**e** and **f**) and 473.15 K (**g** and **h**). CPA-P calculations for H_2O liquid phase (**a**, **c**, **e**, and **g**) and CO_2 gas phase (**b**, **d**, **f**, and **h**). The experimental data points were taken from Malinin (1959); Takenouchi and Kennedy (1965); Toedheide and Franck (1963); Wiebe and Gaddy (1939); Wiebe and Gaddy (1940); Wiebe and Gaddy (1941); Bamberger et al. (2000); Briones et al. (1987); Dohrn et al. (1993); D'souza et al. (1988); Guo et al. (2014); Hou et al. (2013a); Liu et al. (2011); Miiller et al. (1988); Nighswander et al. (1989); Tong et al. (2013).

Fig. 6 (**b**), (**d**), (**f**), and (**h**) show that the calculations of the CPA-P and CPA-WS models are more accurate than PSUCO2 for water content in the carbon dioxide gas phase at 298.15 K to 348.15 K, and 0.1-80 MPa, because the CPA-P and CPA-WS models take into account the interaction of hydrogen bonds between H_2O molecules and CO_2 molecules. Meanwhile, Fig. 6 (**b**) and (**d**) show that the calculations of the PSUCO2 model are below the experimental value at 298.15 K to 308.15 K and 10 to 20 MPa, while Fig. 6 (**h**) indicates that the calculations of the PSUCO2 model are substantially above the experimental value at 348.15 K and 20 to 80 MPa. Fig. 6 (**a**), (**c**), (**e**), and (**g**) show that the calculations of the three models are accurate for carbon dioxide solubility in the H_2O-rich phase at 298.15 K to 348.15 K, and the CPA-P model is the most accurate.

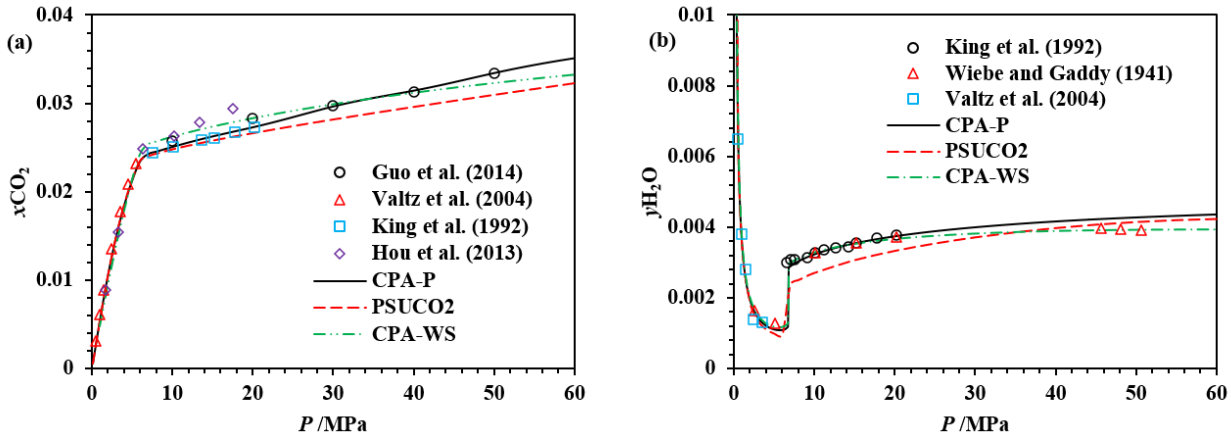

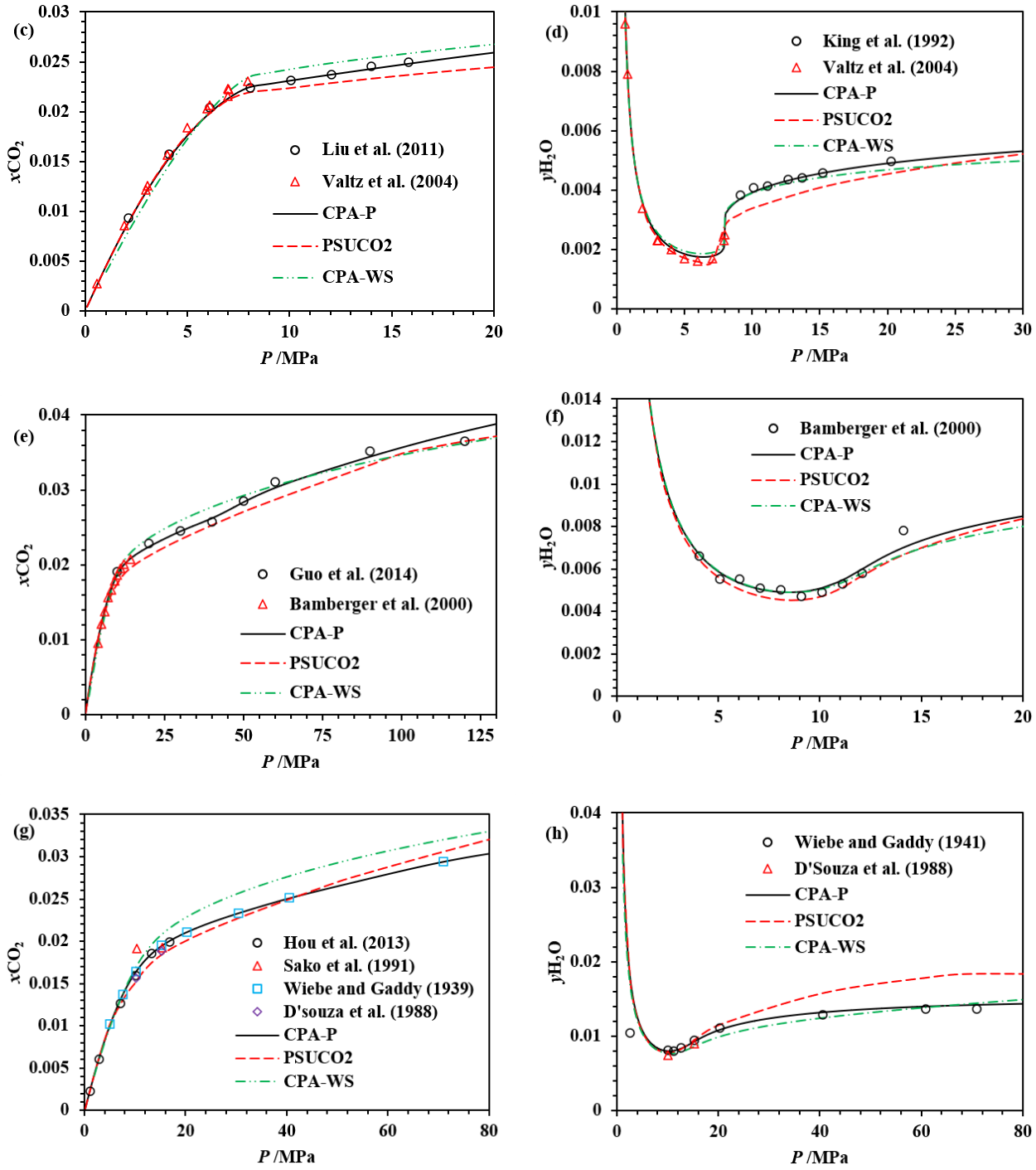

Fig. 6. H_2O-CO_2 VLE at 298.15 K (**a** and **b**), 308.20 K (**c** and **d**), 333.15 K (**e** and **f**), and 348.15 K (**g** and **h**). CPA-P calculations for H_2O liquid phase (**a**, **c**, **e**, and **g**) and CO_2 gas phase (**b**, **d**, **f**, and **h**). The experimental data points were taken from Wiebe and Gaddy (1939); Wiebe and Gaddy (1941); Bamberger et al. (2000); D'souza et al. (1988); Guo et al. (2014); Hou et al. (2013a); King et al. (1992); Liu et al. (2011); Sako et al. (1991); Valtz et al. (2004).

Fig. 7 (**b**), (**d**), (**f**), and (**h**) show that the calculations of the CPA-P model are consistent with the experimental data of water content in carbon dioxide gas phase at 393.15 K to 453.15 K and 0.6 to 6.3 MPa, while the calculations of the PSUCO2 model are slightly below experimental data at 413.15 K to 453.15 K (Fig. 7 **d**, **f**, and **h**). Fig. 7 (**a**), (**c**), (**e**), and (**g**) show that the calculations of the CPA-P model are the most accurate for carbon dioxide solubility in the liquid phase at pressures up to 125 MPa. However, the PSUCO2 and CPA-WS models produce large errors at 433.15 K and above 90 MPa.

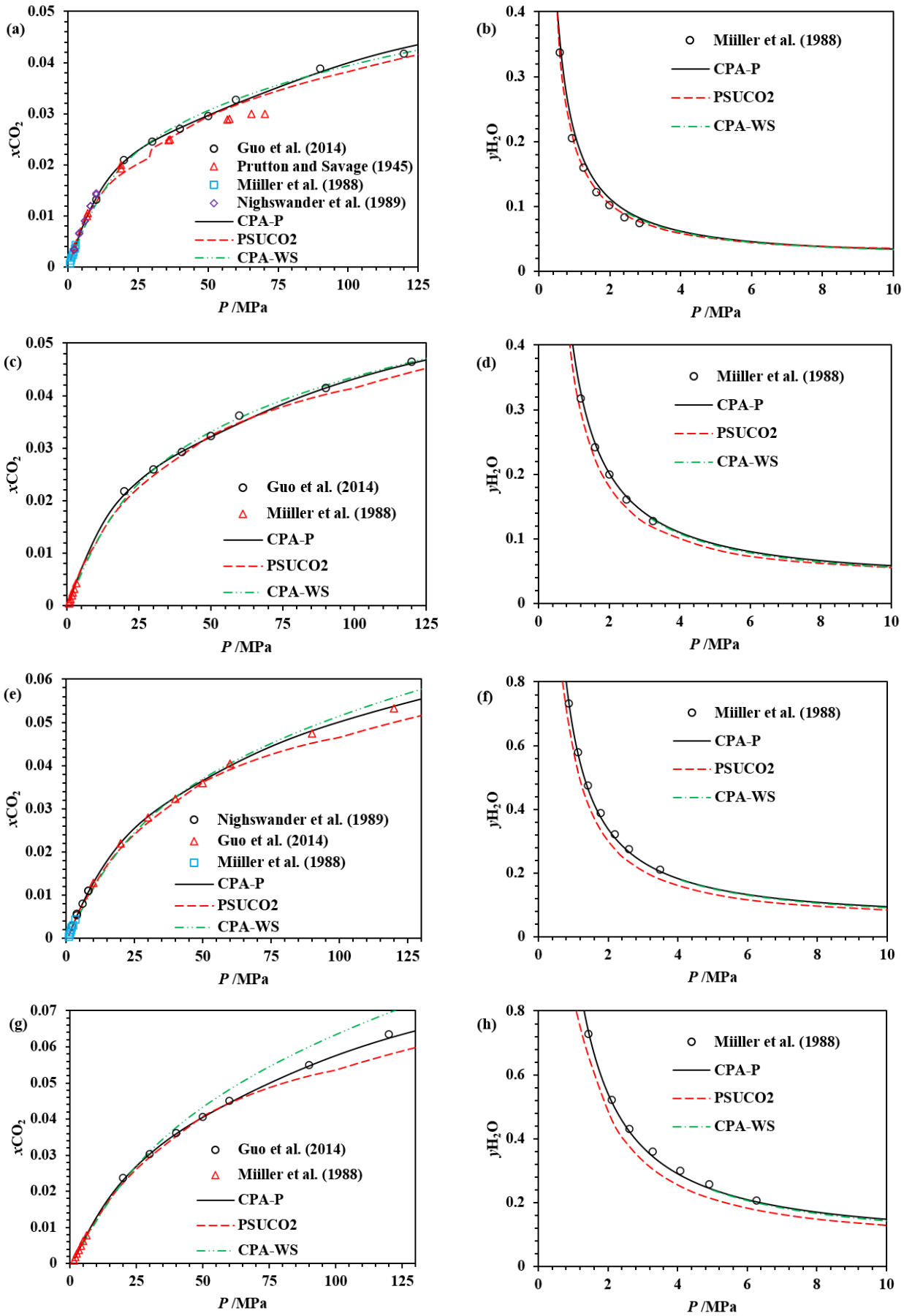

Fig. 7 CO_2-H_2O VLE at 393.15 K (**a** and **b**), 413.15 K (**c** and **d**), 433.15 K (**e** and **f**), and 453.15 K (**g** and **h**). CPA-P calculations for H_2O liquid phase (**a**, **c**, **e**, and **g**) and CO_2 gas phase (**b**, **d**, **f**, and **h**). The experimental data points were taken from Prutton and Savage (1945); Guo et al. (2014); Miiller et al. (1988); Nighswander et al. (1989).

Fig. 8 shows that the calculations of the CPA-P and PSUCO2 models are in agreement with experimental data at 523.15-573.15 K, while the CPA-WS model is not accurate at 523.15 K when the pressure is above 100 MPa (Fig. 8 **a**). Table 6 shows that the average absolute relative deviations (AARDs) of carbon dioxide solubility in the liquid phase of CPA-P, PSUCO2, and CPA-WS models are 3.53%, 5.07%, and 5.14%, and the AARDs of these models for water content in the CO_2-rich phase are 5.83%, 8.77%, and 6.65%, respectively.

$$AARD = \frac{1}{n}\sum_{i=1}^{n}\frac{\left|x_i^{\exp} - x_i^{cal}\right|}{x_i^{\exp}} \quad (21)$$

where x^{exp} is experimental data in mole fraction; x^{cal} is calculated data in mole fraction.

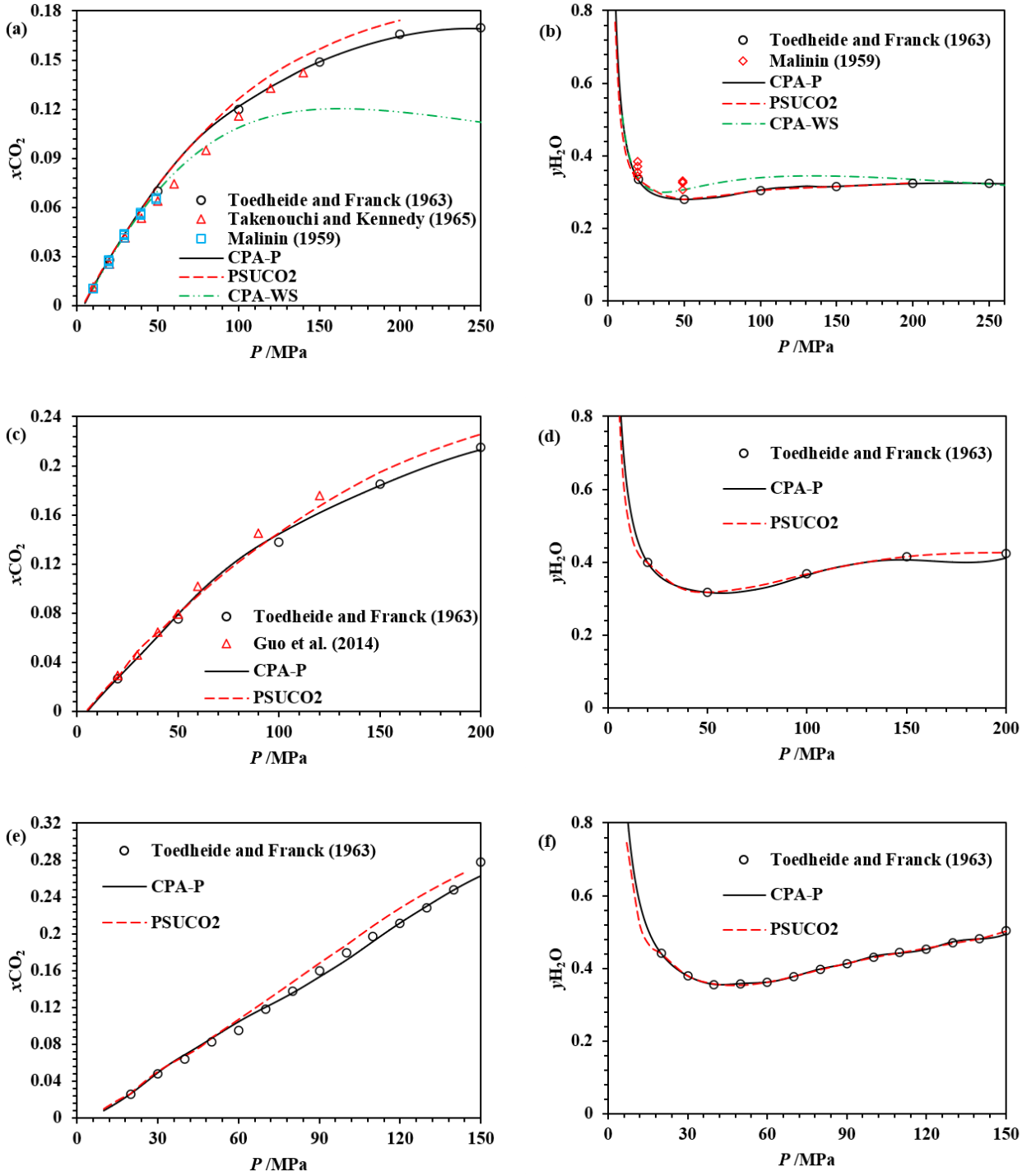

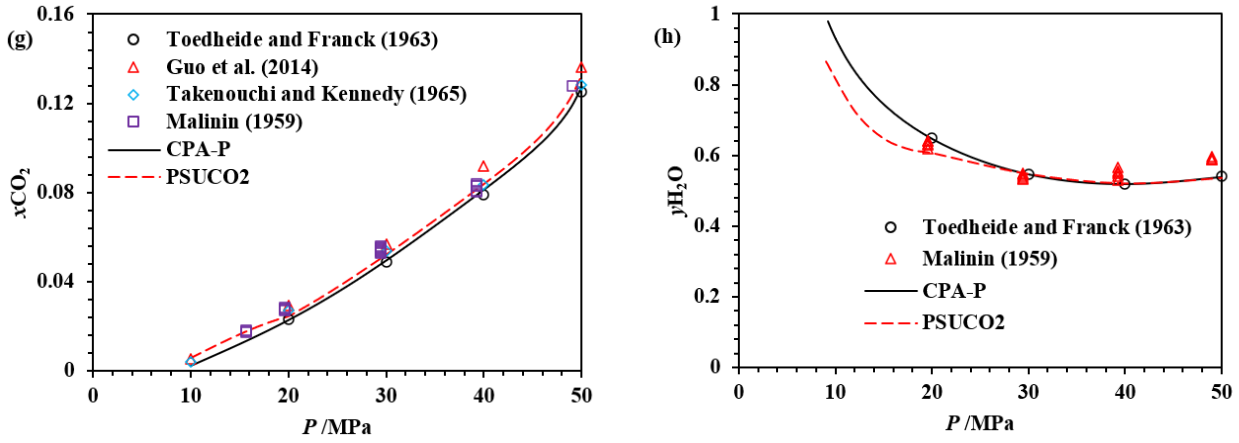

Fig. 8. CO_2-H_2O VLE at 523.15 K (**a** and **b**), 533.15 K (**c** and **d**), 541.15 K (**e** and **f**), and 573.15 K (**g** and **h**). CPA-P calculations for H_2O liquid phase (**a**, **c**, **e**, and **g**) and CO_2 gas phase (**b**, **d**, **f**, and **h**). The experimental data points were taken from Malinin (1959); Takenouchi and Kennedy (1965); Toedheide and Franck (1963); Guo et al. (2014).

4.3. CO_2-H_2O-NaCl system

The PSUCO2 and CPA-WS models are utilized to compare with the CPA-P model for carbon dioxide solubility in brine. The temperature and pressure ranges of the PSUCO2 model are 273.15 to 573.15 K and 0.1 to 200 MPa, while the ranges for the CPA-WS model are 298.15 to 413.15 K and 0.1 to 50 MPa.

Fig. 9 (**a**-**e**) show that the calculations of the CPA-P and PSUCO2 models are more accurate than those of CPA-WS at 313.15-393.15 K, and salinities from 0 to 6 mol·kg^{-1}, and pressures up to 40 MPa. The CPA-WS produces large errors at low molality of NaCl (Fig. 9**a** and **e**). Fig. 9 (**f**-**h**) show that the calculations of the CPA-P model are more accurate than those of PSUCO2 at 423.15-523.15 K and 0.1-140 MPa. The predictions of the PSUCO2 model are above the experimental data at 423.15 K to 523.15 K in Fig. 9 (**f**-**h**).

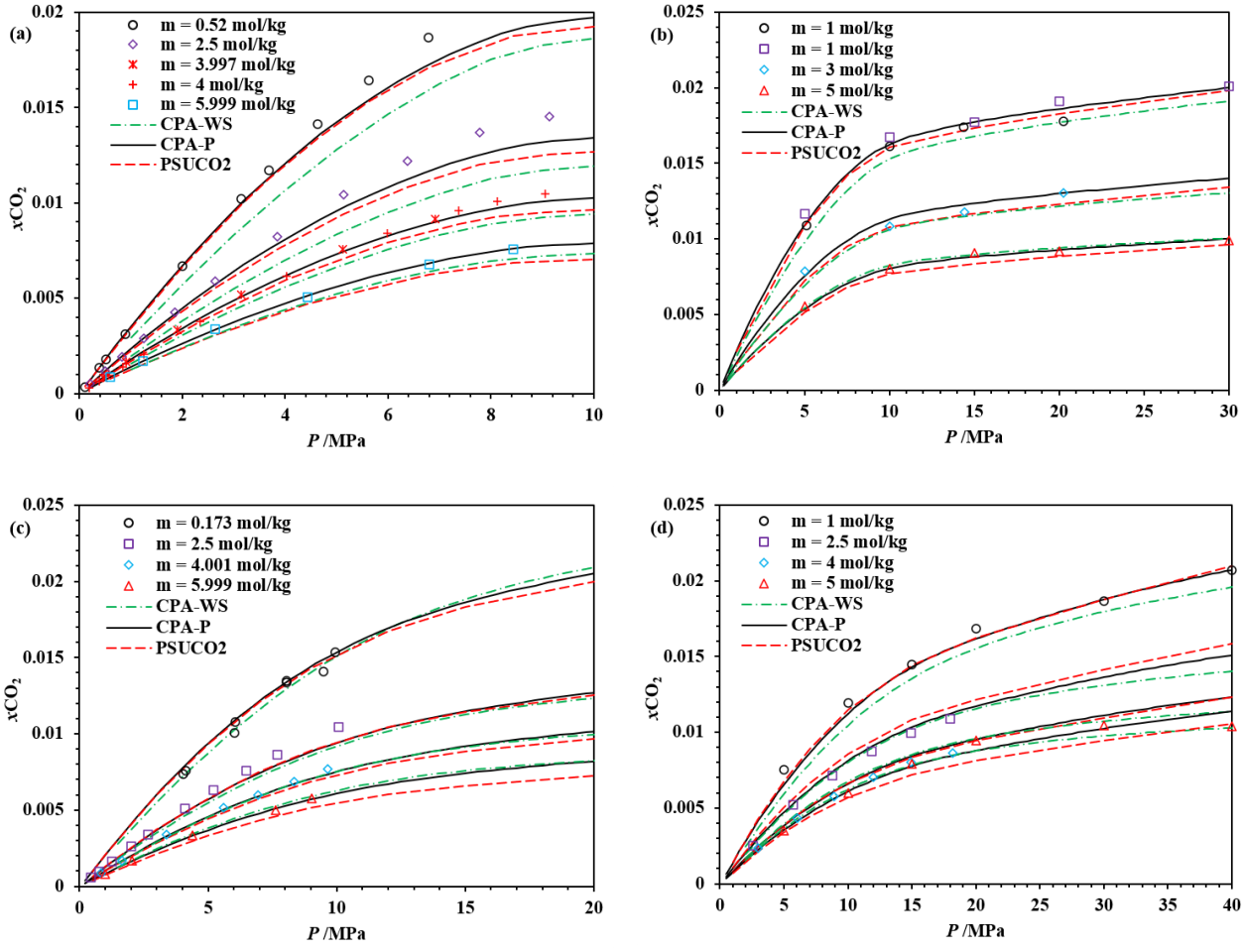

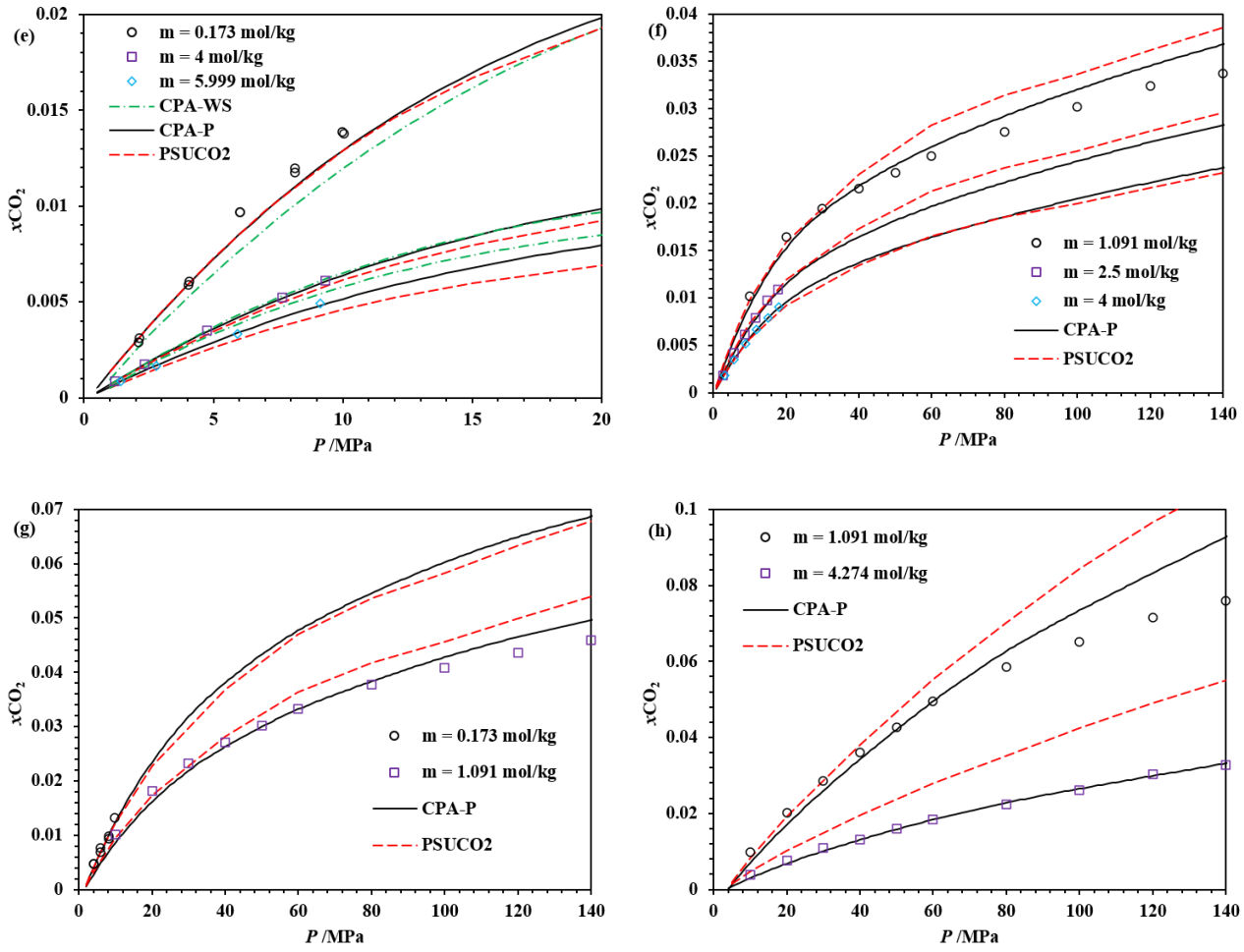

Fig. 9 CO_2-H_2O-NaCl VLE at 313.15 K (**a**), 323.15 K (**b**), 353.15 K (**c**), 373.15 K (**d**), 393.15 K (**e**), 423.15 K (**f**), 473.15 K (**g**) and 523.15 K (**h**). The experimental data points were taken from Takenouchi and Kennedy (1965); Hou et al. (2013b); Kiepe et al. (2002); Koschel et al. (2006); Nighswander et al. (1989); Rumpf et al. (1994); Yan et al. (2011).

Fig. 10 shows that the calculations of CPA-P, PSUCO2, and CPA-WS models for carbon dioxide solubility in brine are accurate at 298.15-423.15 K, 4.795-15.000 MPa, and NaCl molalities of 0–6 mol·kg^{-1}. Fig. 11 shows that the proposed CPA-P model exactly predicts carbon dioxide solubility in aqueous sodium chloride solutions at 273.15-473.15 K, 10-40 MPa, and salinities up to 5 mol·kg^{-1}. Figs. 11 (**a-c**) show that the accuracy of predictions of the CPA-P model is slightly influenced by pressure, especially at 273.15 to 313.15 K. Fig. 12 indicates that the predictions of the CPA-P model for the CO_2-H_2O-NaCl system are consistent with experimental data at 303.15-423.15 K, 0.1-30 MPa, and 0-6 mol·kg^{-1}. However, the predictions of this model are above the experimental data at low temperatures in Figs. 12 (**a**) and (**b**). Table 3 shows that the AARDs of CPA-P, PSUCO2, and CPA-WS models for CO_2 solubility in brine are 3.50%, 4.41%, and 8.38%, respectively.

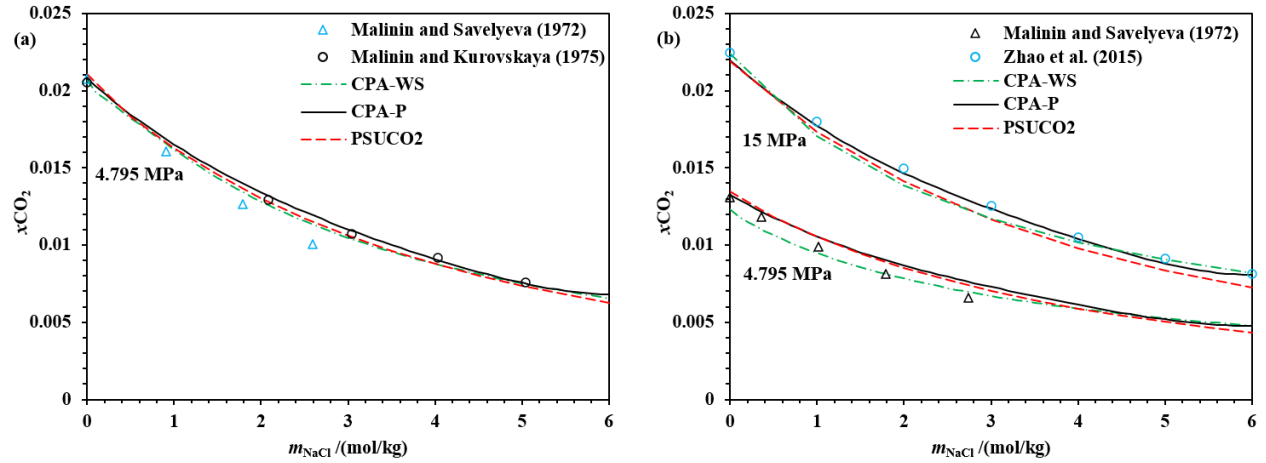

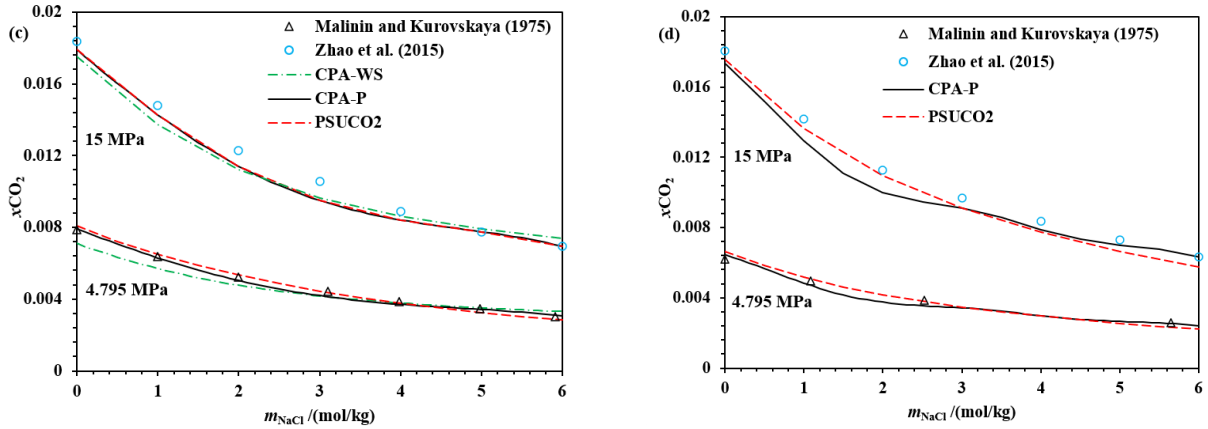

Fig. 10. CO_2-H_2O-NaCl VLE at 298.15 K (**a**), 323.15 K (**b**), 373.15 K (**c**), and 423.15 K (**d**). The experimental data points were taken from Malinin and Kurovskaya (1972); Malinin and Kurovskaya (1975); Zhao et al. (2015).

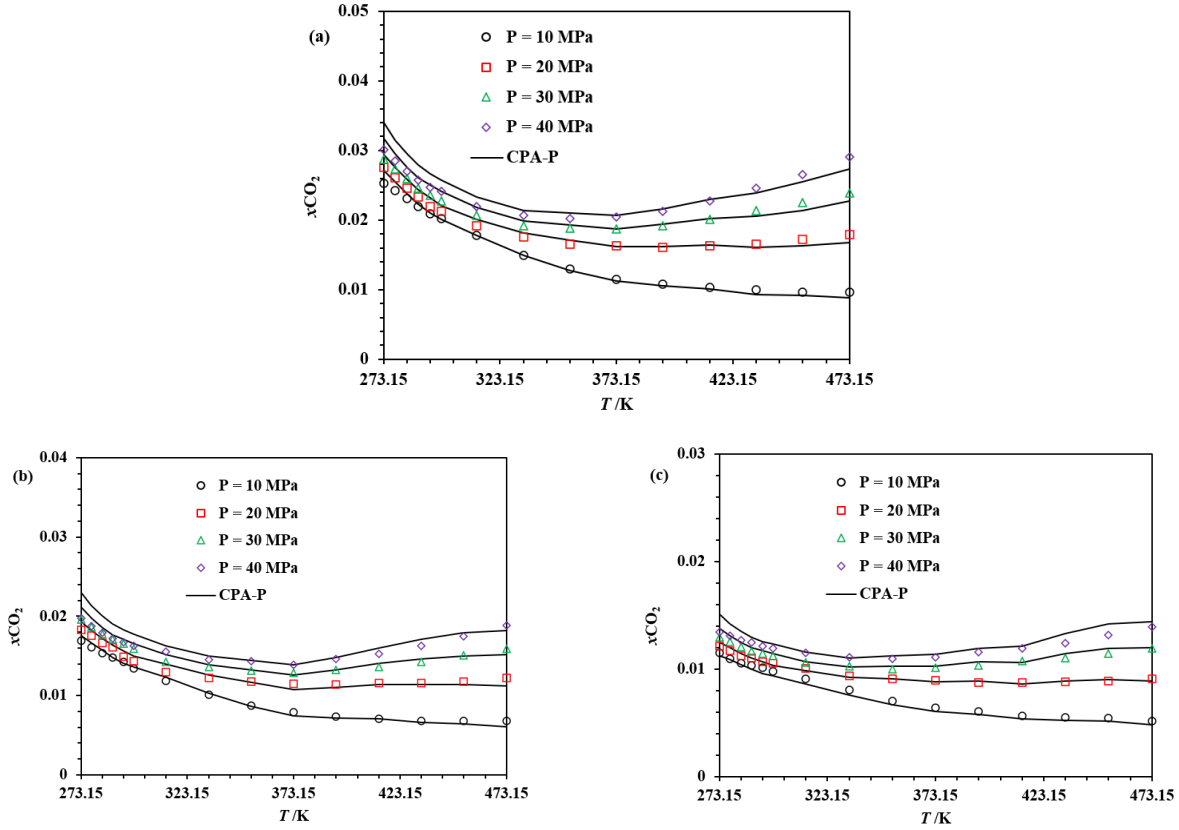

Fig. 11. CO_2-H_2O-NaCl VLE at salinities 1 mol·kg^{-1} (**a**), 3 mol·kg^{-1} (**b**), and 5 mol·kg^{-1} (**c**). CPA-P predictions (black lines). The experimental data points were taken from Guo et al. (2016).

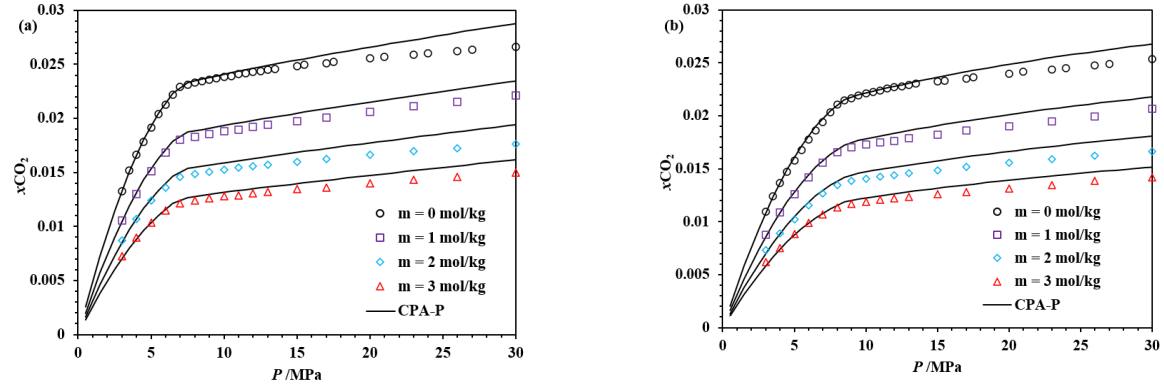

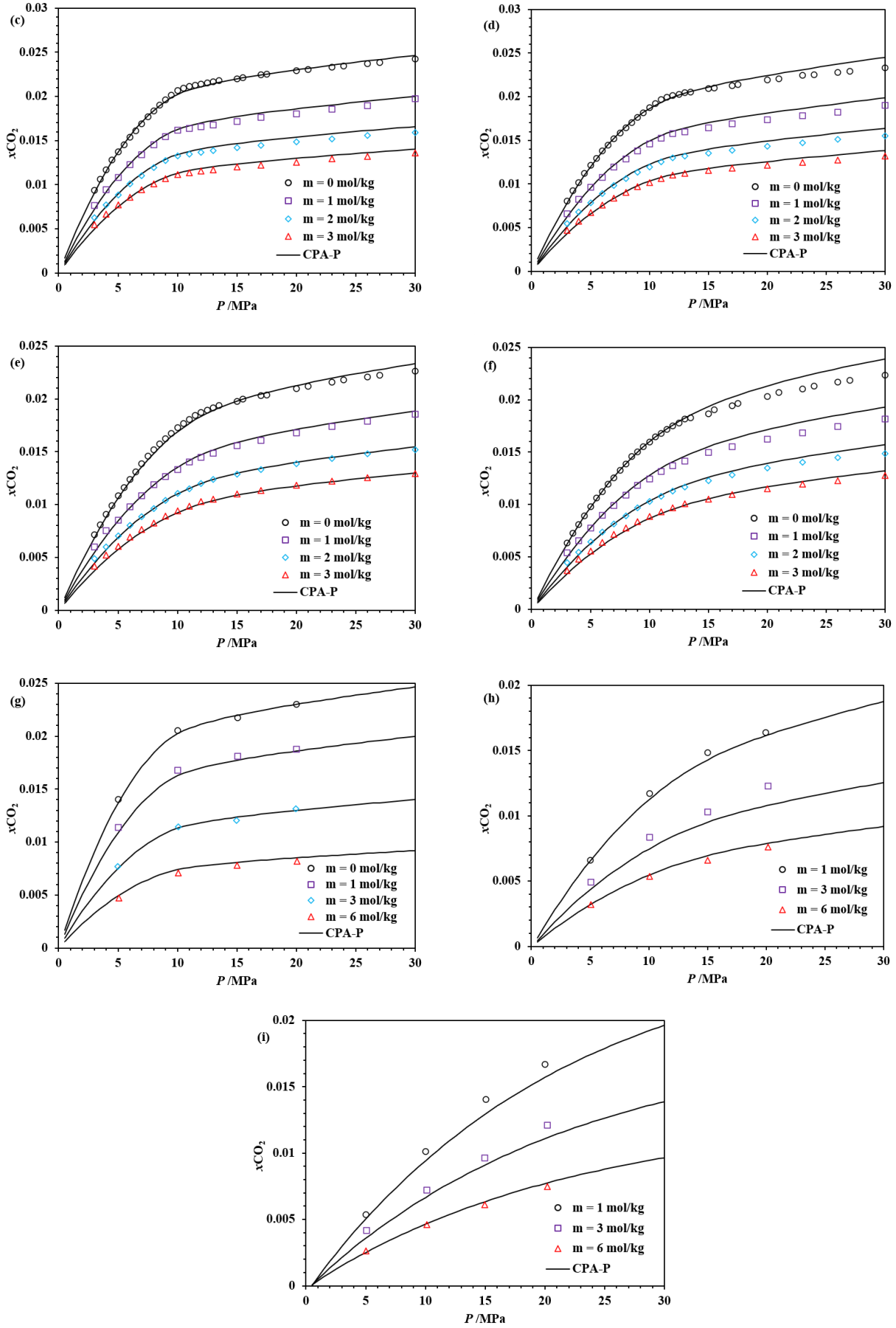

Fig. 12 CO_2-H_2O-NaCl VLE 303.15 K (**a**), 313.15 K (**b**), 323.15 K (**c** and **g**), 333.15 K (**d**), 343.15 K (**e**), 353.15 K (**f**), 373.15 K (**h**) and 423.15 K (**i**). CPA-P predictions (black lines). The experimental data points were taken from Messabeb et al. (2016) and Wang et al. (2019).

The present CPA-P model is parameterized and evaluated for NaCl solutions. Since the aqueous-phase nonideality is described using Pitzer's activity model, the framework can be extended to other electrolyte and mixed-electrolyte systems, such as those containing KCl, $CaCl_2$, and $MgCl_2$, by introducing the corresponding electrolyte interaction parameters. Such an extension requires sufficient experimental data for parameter determination and model evaluation and will be considered in future work.

5. Conclusions

A thermodynamic model (CPA-P) based on the CPA EoS and Pitzer's activity model was constructed to study the phase behavior of the CO_2-H_2O and CO_2-H_2O-NaCl systems over a calculation range of 273.15–573.15 K and 0.1–350 MPa, with NaCl molalities up to 6 mol·kg^{-1} for the brine system. Experimental data for the CO_2-H_2O system extend to 573.15 K and 350 MPa, while those available for the CO_2-H_2O-NaCl system extend to 523.15 K and 140 MPa, with NaCl molalities up to 6 mol·kg^{-1}. The carbon dioxide is considered a pseudo-associating component, and H_2O is modeled using the 4C association scheme. There are five adjustable parameters (i.e., $\overline{v}_{CO_2}$, $k_{CO_2-H_2O}$, $k_{H_2O-CO_2}$, F, and ξ_{nca}) for the CPA-P model, and they are empirically evaluated by fitting experimental data listed in Tables 1-3. Meanwhile, the effect of these parameters was analyzed.

The PSUCO2 and CPA-WS models are utilized for comparison with the CPA-P model. The results of calculations of the CPA-P, PSUCO2, and CPA-WS models for CO_2 solubility in pure H_2O liquid phase are accurate, and the AARDs of them are 3.53%, 5.07%, and 5.14%, respectively. However, the accuracies of the CPA-P and CPA-WS models for water content in the gas phase are above the PSUCO2 model, because the CPA-P and CPA-WS models take into account the interaction of hydrogen bonds between H_2O and CO_2 molecules. And the AARDs of the CPA-P, PSUCO2, and CPA-WS models for water solubility in carbon dioxide gas phase are 5.83%, 8.77%, and 6.65%, respectively.

The calculations of the CPA-P model for CO_2 solubility in brine are accurate at 273.15-523.15 K, 0.1-140 MPa, and 0-6 mol·kg^{-1}. The 376 experimental data points are utilized for correlating the parameter of the CPA-P model, and the AARD of calculations of the CPA-P, PSUCO2, and CPA-WS models for these data are 4.41%, 6.92%, and 7.30%, respectively. Meanwhile, the 724 experimental data points are used to verify the CPA-P model, and the predictions of the CPA-P model are in accordance with these experimental data. The AARD of the predictions of CPA-P, PSUCO2, and CPA-WS models are 3.02%, 3.04%, and 8.87%, respectively. The overall AARD of CPA-P, PSUCO2, and CPA-WS models for CO_2 solubility in brine are 3.50%, 4.41%, and 8.38%, respectively.

Supplementary Materials

The following are available online at: https://serc.yandypress.com/index.php/3104-977X/article/view/142

Author Contributions

W.X., Y.-L.Z., L.-H.Z., S.-M.W., Y.H., H.-B.L., X.H., Y.-C.W.: conceptualization, methodology, software, data curation, writing—original draft preparation, investigation, supervision; X.-Y.L., C.C., T.Z.:software, validation, writing—reviewing and editing. All authors have read and agreed to the published version of the manuscript.

Funding

This research is supported by the State Key Program of National Natural Science Foundation of China (No. U23A2022), State Key Program of National Natural Science Foundation of China (No. 52234003), National Natural Science Foundation of China (No. 52474047, No. 52604057), Sichuan Science and Technology Program (No. 2026NSFSCZY0001), CNPC Innovation Found (2026DQ02030), and National Science and Technology Major Project (No. 2024ZD1406601).

Data Availability Statement

Data will be made available on request.

Acknowledgments

We thank Knut-Andreas Lie, Olav Møyner, and Kai Bao, currently with SINTEF Digital, for helpful technical discussions.

Conflict of interest

The authors declare no conflict of interest.

Use of AI and AI-assisted Technologies

No AI tools were utilized for this paper.

References

Ahmadi, P., Chapoy, A. CO2 solubility in formation water under sequestration conditions. Fluid Phase Equilib., 2018, 463: 80-90.

Akinfiev, N. N., Diamond, L. W. Thermodynamic model of aqueous CO2-H2O-NaCl solutions from -22 to 100 °C and from 0.1 to 100 MPa. Fluid Phase Equilib., 2010, 295: 104-124.

Bamberger, A., Sieder, G., Maurer, G. High-pressure (vapor + liquid) equilibrium in binary mixtures of (carbon dioxide + water or acetic acid) at temperatures from 313 to 353 K. J. Supercrit. Fluids, 2000, 17: 97-110.

Bando, S., Takemura, F., Nishio, M., et al. Solubility of CO2 in aqueous solutions of NaCl at (30 to 60) °C and (10 to 20) MPa. J. Chem. Eng. Data, 2003, 48: 576-579.

Bian, X. Q., Xiong, W., Kasthuriarachchi, D. T. K., et al. Phase equilibrium modeling for carbon dioxide

solubility in aqueous sodium chloride solutions using an association equation of state. Ind. Eng. Chem. Res., 2019, 58: 10570-10578.

Briones, J. A., Mullins, J. C., Thies, M. C., et al. Ternary phase equilibria for acetic acid-water mixtures with supercritical carbon dioxide. Fluid Phase Equilib., 1987, 36: 235-246.

Chabab, S., Théveneau, P., Corvisier, J., et al. Thermodynamic study of the CO2-H2O-NaCl system: Measurements of CO2 solubility and modeling of phase equilibria using Soreide and Whitson, electrolyte CPA and SIT models. Int. J. Greenh. Gas Control, 2019, 91: 102825.

Coelho, F. M., Franco, L. F. M., Firoozabadi, A. Phase equilibria of CO2–water and CO2–brine at high temperatures: from Monte Carlo simulations to the equation of state. Industrial & Engineering Chemistry Research, 2025, 64(16): 8492-8505.

Dohrn, R., Bünz, A. P., Devlieghere, F., et al. Experimental measurements of phase equilibria for ternary and quaternary systems of glucose, water, CO2 and ethanol with a novel apparatus. Fluid Phase Equilib., 1993, 83: 149-158.

D'souza, R., Patrick, J. R., Teja, A. S. High pressure phase equilibria in the carbon dioxiden Hexadecane and carbon dioxide-water systems. Can. J. Chem. Eng., 1988, 66: 319-323.

Duan, Z., Møller, N., Weare, J. H. An equation of state for the CH4-CO2-H2O system: I. Pure systems from 0 to 1000 °C and 0 to 8000 bar. Geochim. Cosmochim. Acta, 1992, 56: 2605-2617.

Duan, Z., Sun, R. An improved model calculating CO2 solubility in pure water and aqueous NaCl solutions from 273 to 533 K and from 0 to 2000 bar. Chem. Geol., 2003, 193: 257-271.

Duan, Z., Sun, R., Zhu, C., et al. An improved model for the calculation of CO2 solubility in aqueous solutions containing Na+, K+, Ca2+, Mg2+, Cl-, and SO2- 4. Mar. Chem, 2006, 98: 131-139.

Fernández, D. P., Goodwin, A. R. H., Lemmon, E. W., et al. A formulation for the static permittivity of water and steam at temperatures from 238 K to 873 K at pressures up to 1200 MPa, including derivatives and Debye-Hückel coefficients. J. Phys. Chem. Ref. Data, 1997, 26: 1125-1166.

Guo, H., Chen, Y., Hu, Q., et al. Quantitative Raman spectroscopic investigation of geo-fluids high-pressure phase equilibria: Part I. Accurate calibration and determination of CO2 solubility in water from 273.15 to 573.15 K and from 10 to 120 MPa. Fluid Phase Equilib., 2014, 382: 70-79.

Guo, H., Huang, Y., Chen, Y., et al. Quantitative Raman spectroscopic measurements of CO2 solubility in NaCl Solution from (273.15 to 473.15) K at p = (10.0, 20.0, 30.0, and 40.0) MPa. J. Chem. Eng. Data, 2016, 61: 466-474.

Hassanzadeh, H., Pooladi-Darvish, M., Elsharkawy, A. M., et al. Predicting PVT data for CO2-brine mixtures for black-oil simulation of CO2 geological storage. Int. J. Greenh. Gas Control, 2008, 2: 65-77.

Hou, S. X., Maitland, G. C., Trusler, J. M. Measurement and modeling of the phase behavior of the (carbon dioxide + water) mixture at temperatures from 298.15 K to 448.15 K. J. Supercrit. Fluids, 2013a, 73: 87-96.

Hou, S. X., Maitland, G. C., Trusler, J. M. Phase equilibria of (CO2 + H2O + NaCl) and (CO2 + H2O + KCl): Measurements and modeling. J. Supercrit. Fluids, 2013b, 78: 78-88.

Ji, X., Tan, S. P., Adidharma, H., et al. SAFT1-RPM approximation extended to phase equilibria and densities of CO2-H2O and CO2-H2O-NaCl systems. Ind. Eng. Chem. Res., 2005, 44: 8419-8427.

Ji, X., Zhu, C. A SAFT equation of state for the quaternary H2S-CO2-H2O-NaCl system. Geochim. Cosmochim. Acta, 2012, 91: 40-59.

Jiang, H., Panagiotopoulos, A. Z., Economou, I. G. Modeling of CO2 solubility in single and mixed electrolyte solutions using statistical associating fluid theory. Geochim. Cosmochim. Acta, 2016, 176: 185-197.

Kiepe, J., Horstmann, S., Fischer, K., et al. Experimental determination and prediction of gas solubility data for CO2 + H2O mixtures containing NaCl or KCl at temperatures between 313 and 393 K and pressures up to 10 MPa. Ind. Eng. Chem. Res., 2002, 41: 4393-4398.

King, M. B., Mubarak, A., Kim, J. D., et al. The mutual solubilities of water with supercritical and liquid carbon dioxides. J. Supercrit. Fluids, 1992, 5: 296-302.

Kontogeorgis, G. M., Michelsen, M. L., Folas, G. K., et al. Ten years with the CPA (Cubic-Plus-Association) equation of state. Part 1. Pure compounds and self-associating systems. Ind. Eng. Chem. Res., 2006a, 45: 4855-4868.

Kontogeorgis, G. M., Michelsen, M. L., Folas, G. K., et al. Ten years with the CPA (Cubic-Plus-Association) equation of state. Part 2. Cross-associating and multicomponent systems. Ind. Eng. Chem. Res., 2006b, 45: 4869-4878.

Kontogeorgis, G. M., Voutsas, E. C., Yakoumis, I. V., et al. An equation of state for associating fluids. Ind. Eng. Chem. Res., 1996, 35: 4310-4318.

Koschel, D., Coxam, J. Y., Rodier, L., et al. Enthalpy and solubility data of CO2 in water and NaCl (aq) at conditions of interest for geological sequestration. Fluid Phase Equilib., 2006, 247: 107-120.

Kurz, F., Rumpf, B., Sing, R., et al. Vapor-liquid and vapor-liquid-solid equilibria in the system ammonia-carbon dioxide-sodium chloride-water at temperatures from 313 to 393 K and pressures up to 3 MPa. Ind. Eng. Chem. Res., 1996, 35: 3795-3802.

Li, D., Duan, Z. The speciation equilibrium coupling with phase equilibrium in the H2O-CO2-NaCl system from 0 to 250 °C, from 0 to 1000 bar, and from 0 to 5 molality of NaCl. Chem. Geol., 2007: 244, 730-751.

Li, Z., Firoozabadi, A. Cubic plus association equation of state for water containing mixtures: Is “cross association” necessary? AIChE J., 2009, 55: 1803-1813.

Liu, Y., Hou, M., Yang, G., et al. Solubility of CO2 in aqueous solutions of NaCl, KCl, CaCl2 and their mixed salts at different temperatures and pressures. J. Supercrit. Fluids, 2011, 56: 125-129.

Malinin, S. D. The system water-carbon dioxide at high temperatures and pressures. Geokhimiya,1959, 3: 292-306.

Malinin, S. D., Kurovskaya, N. A. Solubility of CO2 in chloride solutions at elevated temperatures and CO2 pressures. Geokhimiya, 1975, 4: 547-550.

Malinin, S. D., Savelyeva, N. I. The solubility of CO2 in NaCl and CaCl2 solutions at 25, 50, and 75° under elevated CO2 pressures. Geokhimiya, 1972, 6: 643-653.

Mao, S., Zhang, D., Li, Y., et al. An improved model for calculating CO2 solubility in aqueous NaCl solutions and the application to CO2-H2O-NaCl fluid inclusions. Chem. Geol., 2013, 347: 43-58.

Messabeb, H., Contamine, F., Cézac, P., et al. Experimental measurement of CO2 solubility in aqueous NaCl solution at temperature from 323.15 to 423.15 K and pressure of up to 20 MPa. J. Chem. Eng. Data, 2016, 61: 3573-3584.

Miiller, G., Bender, E., Maurer, G. Vapor-liquid-equilibrium in the ternary-system ammonia-carbon dioxide-water at high water contents in the range 373 K to 473 K. Ber. Bunsen-Ges. Phys. Chem., 1988, 92: 148-160.

Nighswander, J. A., Kalogerakis, N., Mehrotra, A. K. Solubilities of carbon dioxide in water and 1 wt.% sodium chloride solution at pressures up to 10 MPa and temperatures from 80 to 200 ℃. J. Chem. Eng. Data, 1989, 34: 355-360.

Panagiotopoulos, A. Z., Reid, R. C. New mixing rule for cubic equations of state for highly polar, asymmetric systems. Presented at ACS Symposium series 300: American Chemical Society, Washington D.C., 1986.

Pérez-Salado Kamps, Á., Meyer, E., Rumpf, B., et al. Solubility of CO2 in aqueous solutions of KCl and in aqueous solutions of K2CO3. J. Chem. Eng. Data, 2007, 52: 817-832.

Pitzer, K. S. Activity Coefficients in Electrolyte Solutions, second ed. CRC Press, Boca Raton, Ann Arbor, Boston, London 1991.

Pitzer, K. S. Thermodynamics of electrolytes. I. Theoretical basis and general equations. J. Phys. Chem., 1973, 77: 268-277.

Pitzer, K. S., Peiper, J. C., Busey, R. H. Thermodynamic properties of aqueous sodium chloride solutions. J. Phys. Chem. Ref. Data, 1984, 13: 1-102.

Portier, S., Rochelle, C. Modelling CO2 solubility in pure water and NaCl-type waters from 0 to 300 ℃ and from 1 to 300 bar: Application to the Utsira Formation at Sleipner. Chem. Geol., 2005, 217, 187-199.

Prutton, C. F., Savage, R. L. The solubility of carbon dioxide in calcium chloride-water solutions at 75, 100, 120 and high pressures. J. Am. Chem. Soc., 1945, 67: 1550-1554.

Rumpf, B., Maurer, G. An experimental and theoretical investigation on the solubility of carbon dioxide in aqueous solutions of strong electrolytes. Ber. Bunsenges. Phys. Chem., 1993, 97: 85-97.

Rumpf, B., Nicolaisen, H., Öcal, C., et al. Solubility of carbon dioxide in aqueous solutions of sodium chloride: Experimental results and correlation. J. Solut. Chem., 1994, 23: 431-448.

Sako, T., Sugeta, T., Nakazawa, N., et al. Phase equilibrium study of extraction and concentration of furfural produced in reactor using supercritical carbon dioxide. J. Chem. Eng. Jpn., 1991, 24: 449-455.

Salari, H., Hassanzadeh, H., Gerami, S., et al. On estimating the water content of CO2 in equilibrium with formation brine. Pet. Sci. Technol. 2011, 29: 2037-2051.

Shi, X., Mao, S. An improved model for CO2 solubility in aqueous electrolyte solution containing Na+, K+, Mg2+, Ca2+, Cl- and SO2- 4 under conditions of CO2 capture and sequestration. Chem. Geol., 2017, 463: 12-28.

Springer, R. D., Wang, Z., Anderko, A., et al. A thermodynamic model for predicting mineral reactivity in supercritical carbon dioxide: I. Phase behavior of carbon dioxide-water-chloride salt systems across the H2O-rich to the CO2-rich regions. Chem. Geol., 2012, 322: 151-171.

Spycher, N., Pruess, K. A phase-partitioning model for CO2-brine mixtures at elevated temperatures and pressures: Application to CO2-enhanced geothermal systems. Transport in porous media, 2010, 82: 173-196.

Spycher, N., Pruess, K. CO2-H2O Mixtures in the geological sequestration of CO2. II. Partitioning in chloride brines at 12-100 ℃ and up to 600 bar. Geochim. Cosmochim. Acta, 2005, 69: 3309-3320.

Spycher, N., Pruess, K., Ennis-King, J. CO2-H2O mixtures in the geological sequestration of CO2. I. Assessment and calculation of mutual solubilities from 12 to 100 ℃ and up to 600 bar. Geochim. Cosmochim. Acta, 2003, 67: 3015-3031.

Suman, G., Devi, R., Rani, M., et al. Thermodynamic properties of ternary oxygenated fuel mixtures. Journal of Molecular Liquids, 2020, 313: 113541.

Sun, R., Dubessy, J. Prediction of vapor–liquid equilibrium and PVTx properties of geological fluid system with SAFT-LJ EOS including multi-polar contribution. Part I: Application to H2O-CO2 system. Geochim. Cosmochim. Acta, 2010, 74: 1982-1998.

Sun, R., Dubessy, J. Prediction of vapor-liquid equilibrium and PVTx properties of geological fluid system with SAFT-LJ EOS including multi-polar contribution. Part II: Application to H2O-NaCl and CO2-H2O-NaCl System. Geochim. Cosmochim. Acta, 2012, 88: 130-145.

Takenouchi, S., Kennedy, G. C. The solubility of carbon dioxide in NaCl solutions at high temperatures and pressures. Am. J. Sci., 1965, 263: 445-454.

Toedheide, K., Franck, E. U. Two-phase range and the critical curve in the system carbon dioxide-water up to 3500 bar. Z. Phys. Chem., 1963, 37: 387-401.

Tong, D., Trusler, J. M., Vega-Maza, D. Solubility of CO2 in aqueous solutions of CaCl2 or MgCl2 and in a synthetic formation brine at temperatures up to 423 K and pressures up to 40 MPa. J. Chem. Eng. Data, 2013, 58: 2116-2124.

Tsivintzelis, I., Kontogeorgis, G. M., Michelsen, M. L., et al. Modeling phase equilibria for acid gas mixtures using the CPA equation of state. Part II: Binary mixtures with CO2. Fluid Phase Equilib., 2011, 306: 38-

56.

Valtz, A., Chapoy, A., Coquelet, C., et al. Vapour-liquid equilibria in the carbon dioxide-water system, measurement and modelling from 278.2 to 318.2 K. Fluid Phase Equilib., 2004, 226: 333-344.

Verma, S., Gahlyan, S., Rani, M., et al. Transport and acoustic properties of potential renewable oxygenated fuel additives at 308.15 K: butanol isomers+ o-, m-and p-xylene. Journal of Molecular Liquids, 2019, 274: 300-308.

Wagner, W., Pruß, A. The IAPWS formulation 1995 for the thermodynamic properties of ordinary water substance for general and scientific use. J. Phys. Chem. Ref. Data, 2002, 31: 387-535.

Wang, J., He, B., Xie, L., et al. Determination of CO2 solubility in water and NaCl solutions under geological sequestration conditions using a fused silica capillary cell with in situ Raman spectroscopy. J. Chem. Eng. Data, 2019, 64: 2484-2496.

Wiebe, R., Gaddy, V. L. The solubility in water of carbon dioxide at 50, 75 and 100, at pressures to 700 atmospheres. J. Am. Chem. Soc., 1939, 61: 315-318.

Wiebe, R., Gaddy, V. L. The solubility of carbon dioxide in water at various temperatures from 12 to 40 and at pressures to 500 atmospheres. Critical phenomena. J. Am. Chem. Soc., 1940, 62: 815-817.

Wiebe, R., Gaddy, V. L. Vapor phase composition of carbon dioxide-water mixtures at various temperatures and at pressures to 700 atmospheres. J. Am. Chem. Soc., 1941, 63: 475-477.

Wolbach, J. P., Sandler, S. I. Using molecular orbital calculations to describe the phase behavior of cross-associating mixtures. Ind. Eng. Chem. Res., 1998, 37: 2917-2928.

Wong, D. S. H., Sandler, S. I. A theoretically correct mixing rule for cubic equations of state. AIChE J., 1992, 38: 671-680.

Xiong, W., Bian, X. Q., Liu, Y. B. Phase equilibrium modeling for methane solubility in aqueous sodium chloride solutions using an association equation of state. Fluid Phase Equilib., 2020, 506: 112416.

Xiong, W., Zhang, L. H., Tian, Y., et al. Phase equilibrium modeling for carbon dioxide Capture and Storage (CCS) fluids in brine using an electrolyte association equation of state. Chem. Eng. Sci., 2023, 275: 118723.

Xiong, W., Zhang, L. H., Zhao, Y. L., et al. Compositional simulation for carbon storage in porous media using an electrolyte association equation of state. SPE Journal, 2024, 29(6): 3314-3336.

Xiong, W., Zhang, L. H., Zhao, Y. L., et al. EPR-CPA: An electrolyte PR-CPA equation of state for CO2–H2-impurities-brine systems in the geological storage of CO2 and H2. Int. J. Hydrog. Energy, 2025a, 179: 151656.

Xiong, W., Zhang, L. H., Zhao, Y. L., et al. Phase equilibrium modeling for CCUS fluids using a modified association equation of state. The Journal of Supercritical Fluids, 2025b, 219: 106543.

Xiong, W., Zhao, Y. L., Zhang, L. H., et al. Mechanism study of enhanced gas recovery and CO2 storage in naturally fractured carbonate reservoirs using a dual-permeability model coupled with association equation of state. Gas Science and Engineering, 2025c, 139: 205632.

Xu, X., Privat, R., Jaubert, J. N., et al. Phase equilibrium of CCS mixtures: Equation of state modeling and Monte Carlo simulation. J. Supercrit. Fluids, 2017, 119: 169-202.

Yan, W., Huang, S., Stenby, E. H. Measurement and modeling of CO2 solubility in NaCl brine and CO2-saturated NaCl brine density. Int. J. Greenh. Gas Control, 2011, 5: 1460-1477.

Yan, Y., Chen, C. C. Thermodynamic modeling of CO2 solubility in aqueous solutions of NaCl and Na2SO4. J. Supercrit. Fluids, 2010, 55: 623-634.

Zhao, H., Dilmore, R. M., Lvov, S. N. Experimental studies and modeling of CO2 solubility in high temperature aqueous CaCl2, MgCl2, Na2SO4, and KCl solutions. AIChE J., 2015a, 61: 2286-2297.

Zhao, H., Dilmore, R., Allen, D. E., et al. Measurement and modeling of CO2 solubility in natural and synthetic formation brines for CO2 sequestration. Environ. Sci. Technol., 2015b, 49: 1972-1980.

Zhao, H., Fedkin, M. V., Dilmore, R. M., et al. Carbon dioxide solubility in aqueous solutions of sodium chloride at geological conditions: Experimental results at 323.15, 373.15, and 423.15 K and 150 bar and modeling up to 573.15 K and 2000 bar. Geochim. Cosmochim. Acta, 2015c, 149: 165-189.

Zhao, Y., Wang, Y., Wen, S., et al. In-situ experiments of dynamic microscopic reaction for CO2-brine-carbonate system. Chemical Engineering Journal, 2025, 506: 160251.

Ziabakhsh-Ganji, Z., Kooi, H. An Equation of State for thermodynamic equilibrium of gas mixtures and brines to allow simulation of the effects of impurities in subsurface CO2 storage. Int. J. Greenh. Gas Control, 2012, 11S: S21-S34.

Zirrahi, M., Azin, R., Hassanzadeh, H., et al. Mutual solubility of CH4, CO2, H2S, and their mixtures in brine under subsurface disposal conditions. Fluid Phase Equilib., 2012, 324: 80-93.

Zirrahi, M., Azin, R., Hassanzadeh, H., et al. Prediction of water content of sour and acid gases. Fluid Phase Equilib., 2010, 299: 171-179.

Zuo, Z., Lu, P., Zhu, C., et al. SAFT2 equation of state for the CH4–CO2–H2O–NaCl quaternary system with applications to CO2 storage in depleted gas reservoirs. Chemical Geology, 2024, 667: 122328.